frontiers | Frontiers in Genetics

Elucidating the role of pyrabactin-like receptors of finger millet under drought and salinity stress: an insight into *in silico*, machine learning and molecular approaches

Varsha Rani[1,2], Theivanayagam Maharajan[3], Shefali Singh[1],
D. C. Joshi[4]*, Ramwant Gupta[5] and Dinesh Yadav[1]*

[1]Department of Biotechnology, Deen Dayal Upadhyaya Gorakhpur University, Gorakhpur, Uttar Pradesh,
India, [2]Department of Biotechnology, School of Engineering and Technology, Sandip University, Nashik,
Maharashtra, India, [3]Division of Plant Molecular Biology and Biotechnology, Department of Biosciences,
Rajagiri College of Social Sciences, Kochi, Kerala, India, [4]ICAR-Vivekananda Institute of Hill Agriculture,
Almora, Uttarakhand, India, [5]Department of Botany, Deen Dayal Upadhyaya Gorakhpur University,
Gorakhpur, Uttar Pradesh, India

Introduction: The Pyrabactin Resistance 1-like (PYL) receptors, a family of proteins in plants, play a vital role in abscisic acid (ABA) signalling, assisting plants in managing abiotic stresses. Finger millet (*Eleusine coracana* (L.) Gaertn) is a naturally drought tolerant crop, yet the receptor proteins involved in its stress signalling pathways remain poorly understood.

Method: This study employed bioinformatics, machine learning, and molecular approaches to identify, characterize, and profile the expression of PYL receptors in response to drought and salinity stress.

Results: The study identified 14 *PYL* genes in the finger millet genome, irregularly distributed across four of the nine mapped chromosomes. Phylogenetic analysis grouped these genes into three subfamilies. Machine learning analysis highlighted five putative PYL genes—*EcPYL4-2A, EcPYL7-2B, EcPYL11-5A, EcPYL12-5A*, and *EcPYL14-5B* with expression levels exceeding 70% under drought and salinity stress. These genes were further validated through qRT-PCR, confirming their expression under stress conditions, though expression levels varied across tissues and genes.

Discussion: The identification of PYL genes responsive to drought and salt stress provides valuable insights into the stress-signalling mechanisms of finger millet. Among the identified genes, *EcPYL7-2B* and *EcPYL12-5A* emerged as promising candidates for further characterization through genome editing and molecular approaches. This study highlights the potential of these genes in enhancing the stress resilience of finger millet, contributing to its role in improving food and nutritional security under challenging environmental conditions.

KEYWORDS

ABA receptor, ABA signaling pathways, abiotic stress, finger millet, PYL gene family

Introduction

Finger millet (*Eleusine coracana* L. Gaertn.), an ancient grain, has considerable historical, cultural, and nutritional significance, especially in Asia and Africa (Sood et al., 2019). Farmers widely cultivate it in arid and semi-arid regions for their daily diet and to fulfill its nutritional properties for their daily life (Goron and Raizada, 2015). Finger millet is widely recognized for its capacity to thrive in resource-scarce environments and its exceptional nutritional value. Amidst climate change and population expansion, the stability of finger millet production is essential for ensuring global food security and socio-economic development (Rani et al., 2023; Sanjay Kumar et al., 2024).

The growth and yield of finger millet are primarily influenced by biotic and abiotic stresses (Rani et al., 2023). As finger millet has evolved over time, it has developed complex signal networks which regulate a number of biochemical and physiological processes imparting tolerance to biotic and abiotic stresses (Xiong et al., 2002; Hittalmani et al., 2017). Studying the expression pattern and role of key candidate genes associated with stress tolerance will be helpful in developing new stress responsive finger millet genotypes.

Abscisic acid (ABA) is a phytohormone that has a huge impact on plant development and growth. It is an important hormone that controls organ senescence and morphogenesis, stomatal movement, and transpiration (Cutler et al., 2010; Zhu, 2016). In addition to acting as a stress indicator for plants, ABA may also be used to identify drought, salinity, or pathogen infection (Zhu, 2002; Cutler et al., 2010). In response to abiotic stress, the accumulation of ABA increases in plants. Generally, plants perceive ABA through the Pyrabactin Resistance 1 (PYR1)/PYR1-like (PYL)/Regulatory component of the ABA receptor (RCAR) protein family. After binding to PYL, ABA changes the conformation of PYL, which facilitates its binding to type 2C protein phosphatases (PP2Cs). This allows SnRK2s to be released from PP2C inhibition. Yadav et al. (2020) reported that ABA stimulates downstream targets like transcription factors (TF) and other regulatory proteins because it turns on SnRK2. The stimulated TF then enters the nucleus, up-regulating downstream genes associated with ABA-induced stress. Hence, land plants require PYLs, PP2Cs, and SnRK2s for ABA signalling to survive under abiotic stresses like drought, salinity, and others (Cutler et al., 2010).

PYLs have been identified and characterized in *Arabidopsis* (Gonzalez-Guzman et al., 2012), rice (Kim et al., 2012; Yadav et al., 2020), sorghum (Dalal and Inupakutika, 2014), maize (Fan et al., 2018; Wang et al., 2018) and wheat (Lei et al., 2021). Some plants, like *Arabidopsis*, have a gene called AtPYR1 that codes for a cyclase subfamily member and is part of the star related lipid transfer (START) domain superfamily (Park et al., 2009). *AtPYL* (PYR1-like) genes *AtPYL1* to *AtPYL13* are genes that share the same function as *AtPYR1*. In *Arabidopsis* PYL family, there are 14 members, each having a START domain. These 14 PYLs are divided into three subfamilies (Park et al., 2009; Park et al., 2010). It has been observed that some *AtPYLs* form monomers which interact with phosphatase 2C (Bai et al., 2013) protein without the involvement of ABA. In addition, some *AtPYLs* can form homodimers that only interact with PP2C after binding to ABA (Hao et al., 2011). It has been reported that overexpression of AtPYL4 enhanced drought tolerance in *Arabidopsis*. More interestingly, overexpression of OsPYL5 in rice improved drought and salinity tolerance (Pizzio et al., 2013; Kim et al., 2014). These results suggest that the PYL family plays an important role in plant development and abiotic stress response. However, the role of PYL receptors in finger millet under abiotic stresses is still unknown, and needs to be deciphered. Identification and characterization of *PYL* genes across the finger millet genome can provide an insight into the response of finger millet towards stresses and role of ABA signaling pathways.

Several studies have reported that finger millet is drought-tolerant, yet further research is required to identify how genes and regulatory proteins contribute to stress impartation in finger millet (Mukami et al., 2019; Talwar et al., 2020; Rani et al., 2024a; Rani et al., 2024c; Rani et al., 2024b). The draft and annotated genome sequence of finger millet has been made public and openly accessible (Hittalmani et al., 2017; Hatakeyama et al., 2018); however, many genes are still unannotated and need to be studied using *in silico* and wet lab methods. To the best of our knowledge, the role of PYL receptors in finger millet, has not been reported. The ultimate aim of the study is to reveal the role of PYL receptors in finger millet through *in silico*, machine learning and molecular approaches.

The advancement of bioinformatics and computational tools has enabled the integration of machine learning (ML) into stress biology, offering new opportunities for predicting gene expression patterns under adverse environmental conditions. This study provides an insight into the role of Pyrabactin-Like Receptors (PYL) in finger millet under drought and salinity stress with involvement of ABA signaling pathways using a comprehensive approach comprising of *in silico*, machine learning, and molecular tools. The finger millet genome was mined for several bioinformatics attributes like phylogenetic analysis, chromosomal localization, gene structure mapping, motif analysis, cis-regulatory element identification, protein-protein interaction analysis, miRNA target predictions and digital expression profiling using machine learning algorithm of ASRpro web server (Meher et al., 2024). Further, the most promising PYL candidate genes, likely to be expressed under drought and salinity stress, has been identified revealing the possible plant stress adaptation mechanisms. Furthermore, qRT-PCR validation was conducted for the identified candidate genes in shoots and roots of finger millet exposed to drought and salinity stress. The identification of key PYL receptors in finger millet could reveal the possible molecular mechanisms underlying its resilience to abiotic stresses.
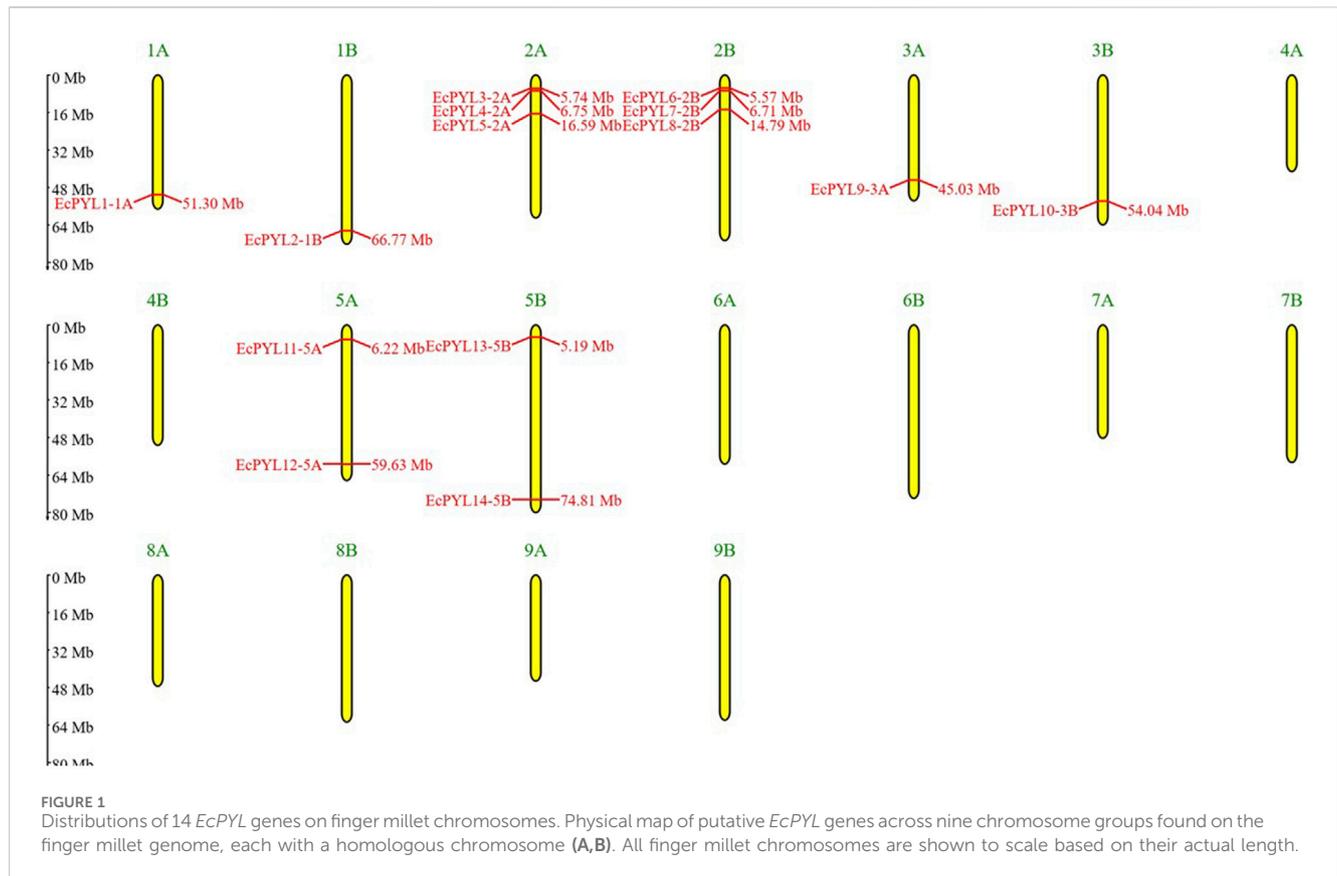

TABLE 1 Details of primers used for qRT-PCR analysis.

S. no.	Gene name	Forward primer	Reverse primer	Product size with intron	Product size without intron	Annealing temperature (°C)
1	*EcPYL4-2A*	ACCTCGTTTGGT CTCTGGTG	TCGATGATCACC TCCAACAA	-	215	60.0
2	*EcPYL7-2B*	CCTGCTACACGA AGCACTGA	CGACTTGAGGTT GCACTTGA	1,284	249	60.1
3	*EcPYL11-5A*	GGATCACCACCA TCACGAG	CTCCGGATGAAG TGCTTGTA	-	214	59.2
4	*EcPYL12-5A*	ACCGCCTCCAGA ACTACTCA	CCTCGACGAAGT AGCAGGTC	-	141	59.9
5	*EcPYL14-5B*	CACCGCCTCCAG AACTACTC	CTGCAAGAGACG TGAGGTTG	-	175	59.7

TABLE 2 Gene position, ORF length, domain position and chromosome location of putative *PYLs* genes of finger millet.

NCBI Acc. no.	Transcript name	Gene name	Gene start (bp)	Gene end (bp)	Chromosome name	ORF length (bp)	PFAM ID	PFAM description	Domain position HMM SCAN
GJM92688.1	ELECO.r07.1AG0038470.1	*EcPYL1-1A*	51,299,793	51,300,389	1A	597	PF10604	Polyketide_cyc2	47–194
GJN17299.1	ELECO.r07.1BG0088430.1	*EcPYL2-1B*	66,773,446	66,774,072	1B	627	PF10604	Polyketide_cyc2	56–204
GJN19381.1	ELECO.r07.2AG0106820.1	*EcPYL3-2A*	5,737,836	5,738,444	2A	609	PF10604	Polyketide_cyc2	38–187
GJN19492.1	ELECO.r07.2AG0108140.1	*EcPYL4-2A*	6,745,596	6,748,419	2A	636	PF10604	Polyketide_cyc2	53–198
GJM91546.1	ELECO.r07.2AG0117770.1	*EcPYL5-2A*	16,588,979	16,589,524	2A	546	PF10604	Polyketide_cyc2	15–165
GJM90649.1	ELECO.r07.2BG0160340.1	*EcPYL6-2B*	5,566,370	5,566,972	2B	603	PF10604	Polyketide_cyc2	38–185
GJN19492.1	ELECO.r07.2BG0161780.1	*EcPYL7-2B*	6,714,154	6,716,983	2B	639	PF10604	Polyketide_cyc2	54–199
GJN20187.1	ELECO.r07.2BG0171370.1	*EcPYL8-2B*	14,790,778	14,791,404	2B	627	PF10604	Polyketide_cyc2	41–192
GJN08144.1	ELECO.r07.3AG0244730.1	*EcPYL9-3A*	45,026,141	45,026,809	3A	669	PF10604	Polyketide_cyc2	70–216
GJN31193.1	ELECO.r07.3BG0283350.1	*EcPYL10-3B*	54,043,193	54,043,861	3B	669	PF10604	Polyketide_cyc2	70–216
GJM88866.1	ELECO.r07.5AG0369710.1	*EcPYL11-5A*	6,215,159	6,215,770	5A	612	PF10604	Polyketide_cyc2	51–196
GJM94889.1	ELECO.r07.5AG0401550.1	*EcPYL12-5A*	59,625,111	59,626,595	5A	627	PF10604	Polyketide_cyc2	50–196
GJN14692.1	ELECO.r07.5BG0417310.1	*EcPYL13-5B*	5,193,046	5,193,648	5B	603	PF10604	Polyketide_cyc2	48–193
GJN35776.1	ELECO.r07.5BG0450090.1	*EcPYL14-5B*	74,809,940	74,811,451	5B	597	PF10604	Polyketide_cyc2	50–196

FIGURE 1
Distributions of 14 *EcPYL* genes on finger millet chromosomes. Physical map of putative *EcPYL* genes across nine chromosome groups found on the finger millet genome, each with a homologous chromosome **(A,B)**. All finger millet chromosomes are shown to scale based on their actual length.

Materials and methods

Collection and characterization of *PYL* genes of finger millet

Firstly, we obtained the PYL full-length protein sequence of rice from the NCBI (http://www.ncbi.nlm.nih.gov/nucleotide/) (Yadav et al., 2020). The rice *PYLs* gene sequences were used as query sequences in the Phytozome database (https://phytozome-next.jgi.doe.gov/) to find PYLs in the finger millet genome. This was done by using BLASTp searches (http://blast.ncbi.nlm.nih.gov/) against the finger millet genome *E. coracana* v1.1 (Goodstein et al., 2012; Hittalmani et al., 2017; Hatakeyama et al., 2018). The appeared duplicate and redundant sequences were eliminated by venny2.1 (https://bioinfogp.cnb.csic.es/tools/venny/) (Oliveros, 2016). Then, the NCBI open reading frames (ORF) Finder (http://www.ncbi.nlm.nih.gov/gorf/gorf.html) was used to determine ORFs. On the other hand, we used Pfam (https://www.ebi.ac.uk/interpro/entry/pfam/) to search for the polyketide cyclase 2/START domain (PF10604), which is a characteristic of the PYR/PYL protein sequence. Further, multiple sequence alignment by MEGA11 was used to identify conserved amino acid residues among all putative PYL sequences of finger millet (Tamura et al., 2021). Genes that lack specific conserved domains were sorted and removed. Further the domain position, physicochemical attributes and subcellular localization were predicted by HMMSCAN (http://www.ebi.ac.uk/Tools/hmmer/search/hmmscan, ExPaSy Protparam (https://web.expasy.org/protparam/) and Wolf-Psort online tool (https://www.genscript.com/tools/wolf-psort) respectively (Gasteiger et al., 2005; Horton et al., 2007).

Evolutionary analysis, gene structure display and motif prediction of *PYL* genes

The *PYL* gene family in finger millet has been designated as EcPYL1-1A, which indicates for the first *PYL* genes of *E. coracana* and is found on chromosome 1A. Similarly, other finding was also annotated and used for evolutionary study. An evolutionary analysis was made between putative *PYLs* genes of finger millet and the *PYLs* genes of rice (Yadav et al., 2020), sorghum (Dalal and Inupakutika, 2014), and foxtail millet (Duarte et al., 2019), which were retrieved from the Phyozome and NCBI database. All of the retrieved sequences of the *PYL* genes family were aligned through ClustalW, and the phylogenetic tree was constructed through MEGA11 using the Maximum Likelihood method at 1,000 bootstrap levels (Larkin et al., 2007; Tamura et al., 2021). MapGene2 Chromosome v2.1 (http://mg2c.iask.in/mg2c_v2.1/) was used for physical mapping of *PYLs* gene of finger millet (Devos et al., 2023), and TB tool was used to display the exon-intron structure (Chen et al., 2020; Chao et al., 2021). The MEME Suite Vs. 5.5.3 (https://meme-suite.org/meme/tools/meme) predicted the conserved motif within each finger millet protein sequence. The maximum number of motifs was set to 6, keeping others at default parameters (Bailey et al., 2015).

TABLE 3 Physicochemical attributes of putative PYL receptor proteins of finger millet.

EcPYL receptors	NCBI accession no.	No. of amino acids	Molecular weight (dalton)	PI value	Richness in amino acid	Total number of negatively charged residues (Asp + Glu)	Total number of positively charged residues (Arg + Lys)	Instability index	Aliphatic index	GRAVY	Subcellular localization
EcPYL1-1A	GJM92688.1	198	21150.91	8.65	Val (V)	20	23	55.52	85.51	−0.078	Cytoplasmic
EcPYL2-1B	GJN17299.1	208	22221.21	9.03	Val (V)	20	25	51.94	83.32	−0.079	Chloroplast
EcPYL3-2A	GJN19381.1	202	21950.57	6.55	Val (V)	24	22	41.5	76.63	−0.361	Cytoplasmic
EcPYL4-2A	GJN19492.1	211	23667.91	6.25	Val (V)	33	30	49.22	87.68	−0.394	Cytoplasmic
EcPYL5-2A	GJM91546.1	181	19497.12	6.2	Ala (A)	21	19	43	92.15	−0.117	Chloroplast
EcPYL6-2B	GJM90649.1	200	21688.29	6.38	Val (V)	24	22	45.97	76.9	−0.335	Cytoplasmic
EcPYL7-2B	GJN19492.1	212	23696.91	6.08	Val (V)	33	29	49.62	87.26	−0.39	Cytoplasmic
EcPYL8-2B	GJN20187.1	208	22277.03	5.5	Ala (A)	26	20	41.24	87.26	−0.218	Cytoplasmic
EcPYL9-3A	GJN08144.1	222	23204.15	6.58	Ala (A)	21	19	45.74	79.95	−0.05	Chloroplast
EcPYL10-3B	GJN31193.1	222	23181.11	6.54	Ala (A)	21	19	47.14	79.95	−0.052	Chloroplast
EcPYL11-5A	GJM88866.1	203	22052.87	8.72	Val (V)	21	24	44.1	84.98	−0.184	Chloroplast
EcPYL12-5A	GJM94889.1	208	22416.44	6.13	Val (V)	26	22	41.24	94.52	−0.128	Cytoplasmic
EcPYL13-5B	GJN14692.1	200	21586.24	8.36	Val (V)	21	23	47.94	83.3	−0.2	Chloroplast
EcPYL14-5B	GJN35776.1	198	21414.34	6.3	Val (V)	25	22	38.38	90.96	−0.152	Cytoplasmic

FIGURE 2
Evolutionary analysis and gene structure organizations of *EcPYL* genes, Exons and introns are represented by maroon boxes and blue lines, respectively. Scale represents the sizes of exons and introns.
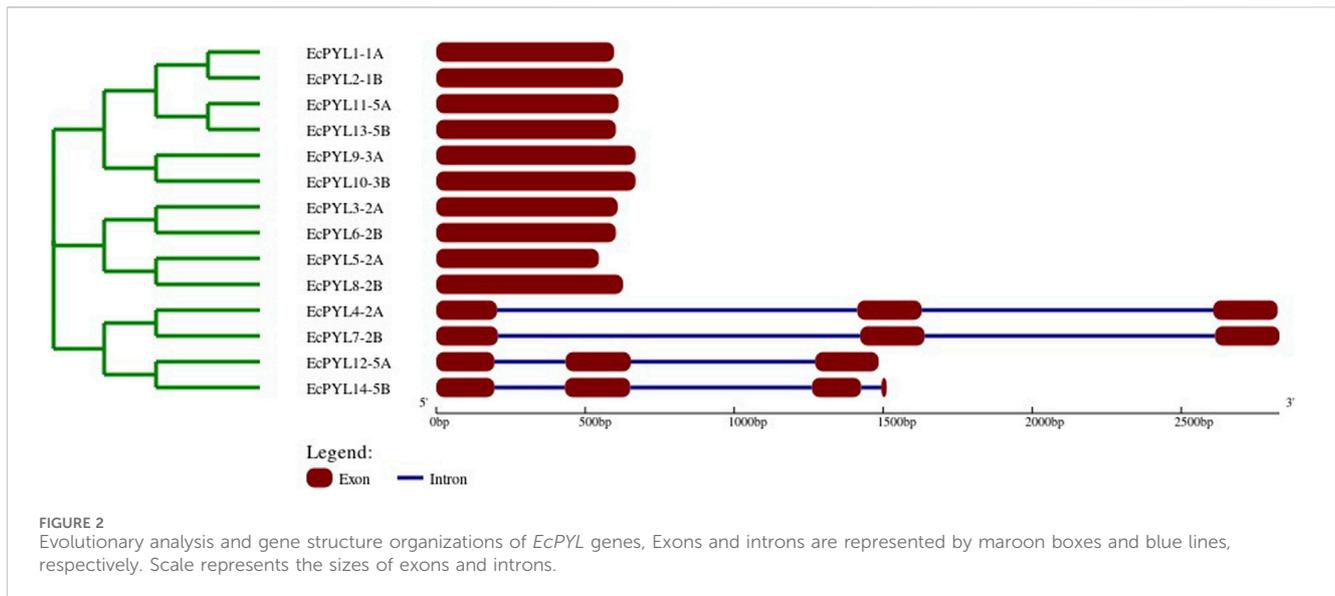
Ka/Ks and gene duplication analysis of *PYLs* gene family of finger millet

A ratio of non-synonymous (Ka) versus synonymous (Ks) substitution rates of nucleotides was calculated among finger millet *PYLs* gene family by using Ka/Ks calculation tool (http://services.cbu.uib.no/tools/kaks) and the gene duplication event was calculated by using T = Ks/2λ, where (λ)= (6.5×10^{-9} (Gaut et al., 1996; Zhang et al., 2006). It measures the selective pressures placed on genes and can be used to identify pairs of genes where encoded proteins may have changed their function. When the ratio of Ka/Ks > 1, it indicates that there is a positive selective pressure or Darwinian selection. If the ratio is 1, it indicates neutral evolution and if the ratio is less than 1, then it indicates stabilizing selection, i.e., the protein sequence is pressured to be conserved.

Prediction of cis-regulatory elements in the promoters of finger millet

The 2,000 bp upstream sequences from the translations tart site of all of the *EcPYLs* genes were obtained from finger millet genome at Phytozome database (Goodstein et al., 2012) and the putative cis regulatory elements were predicted by using the PlantCARE web server (http://bioinformatics.psb.ugent.be/webtools/plantcare/html/) to know the putative function associated with the genes (Lescot et al., 2002). According to the cis-regulatory elements, *PYL* genes were categorized into three groups based on their response to phytohormones, stress, and growth and development.
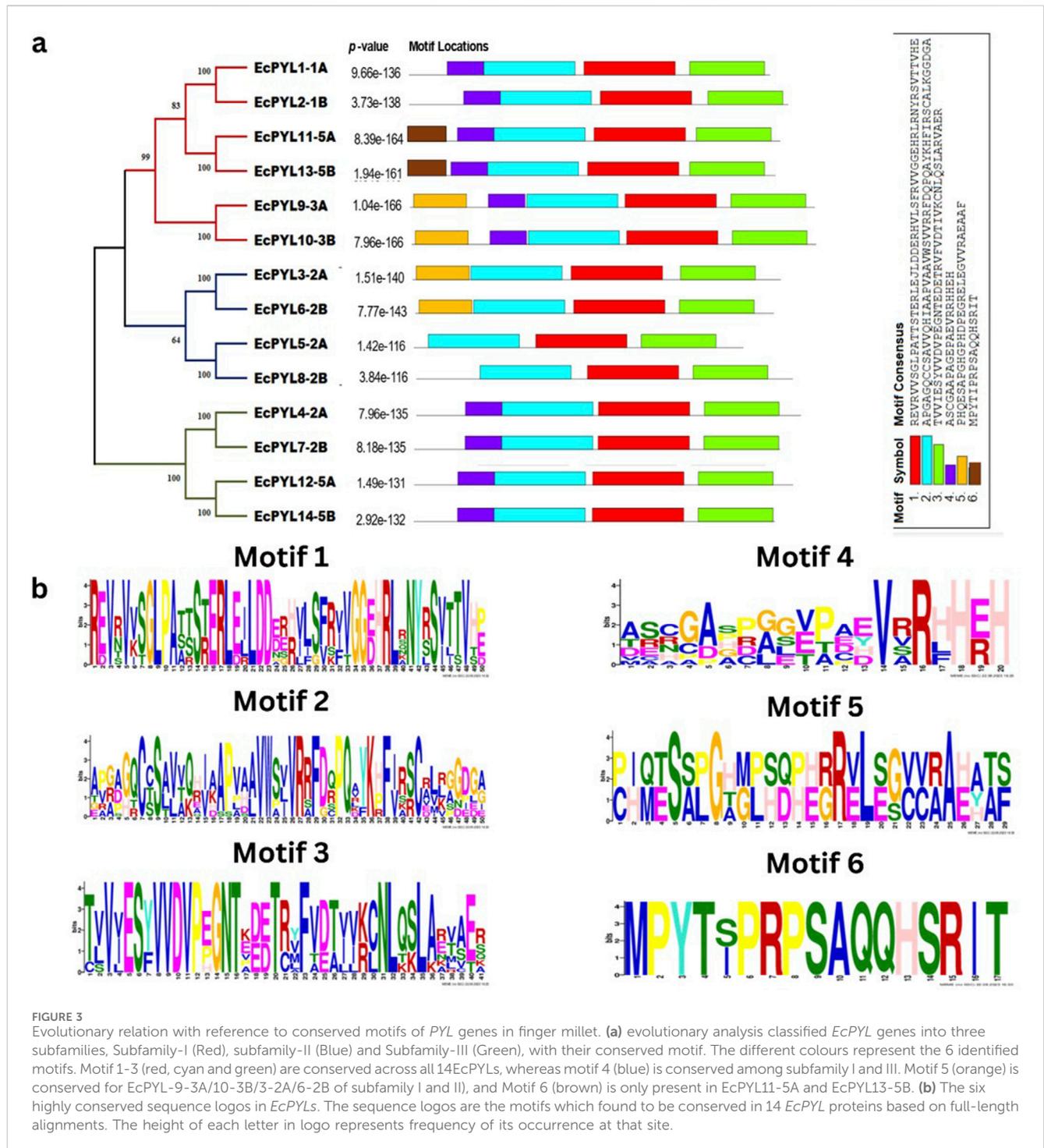
miRNA-PYLs target prediction and protein-protein interaction and gene ontology analysis

For the prediction of miRNA target sites in the *EcPYL* genes, the miRNA dataset of finger millet was retrieved from

PmiREN server (https://www.pmiren.com/) (Guo et al., 2020) and cDNA sequence of *EcPYLs* genes were examined against miRNA dataset using the pSRNATarget server (https://www.zhaolab.org/psRNATarget/) (Dai and Zhao, 2011). To determine the interrelationships among the 14 putative *EcPYLs* genes, the STRING database (https://string-db.org/) (Szklarczyk et al., 2021) was used at confidence level (0.07) against rice (Yu et al., 2002), *Arabidopsis* (Cheng et al., 2017), sorghum (McCormick et al., 2018) and foxtail millet (Zhang et al., 2012) genome one by one. Using the combination of Cytoscape v. 3.10.3 with MCODE (Molecular Complex Detection), the most accurate prediction of the interaction network was displayed. Additionally, the integration of Cytoscape v. 3.10.3 with BinGO program were used for Gene Ontology (GO), functional annotation and gene enrichment profiling of *EcPYL* genes of finger millet (Paul et al., 1971; Bader and Hogue, 2003).

Machine learning approach for preselection of candidate genes

After characterization of *EcPYL* genes, machine learning algorithm was used to predict the expression pattern of these genes. For the prediction of probability of expression of *EcPYL* genes under drought and salinity stresses we used ASRPro webserver (http://iasri-sg.icar.gov.in/asrpro/result.php) (Meher et al., 2024). This web server utilized machine learning algorithms to assess the likelihood of gene expression under the given stress conditions, and generated a probability score for each gene. Genes with a probability score of ≥0.70 were considered highly likely to be expressed in response to drought and salinity stress. On the basis of the probability of gene expression, we constructed a heatmap and scatter plot to predict the candidate genes for qRT-PCR expression profiling.

FIGURE 3
Evolutionary relation with reference to conserved motifs of *PYL* genes in finger millet. **(a)** evolutionary analysis classified *EcPYL* genes into three subfamilies, Subfamily-I (Red), subfamily-II (Blue) and Subfamily-III (Green), with their conserved motif. The different colours represent the 6 identified motifs. Motif 1–3 (red, cyan and green) are conserved across all 14EcPYLs, whereas motif 4 (blue) is conserved among subfamily I and III. Motif 5 (orange) is conserved for EcPYL-9-3A/10-3B/3-2A/6-2B of subfamily I and II), and Motif 6 (brown) is only present in EcPYL11-5A and EcPYL13-5B. **(b)** The six highly conserved sequence logos in *EcPYLs*. The sequence logos are the motifs which found to be conserved in 14 *EcPYL* proteins based on full-length alignments. The height of each letter in logo represents frequency of its occurrence at that site.

Gene expression analysis

Five *PYL* genes (*EcPYL4-2A, EcPYL7-2B, EcYL11-5A, EcPYL12-5A,* and *EcPYL14-5B*) with probability score of 0.70 were selected for qRT-PCR analysis. Primers for each gene were designed using Primer3 input software (https://bioinfo.ut.ee/primer3-0.4.0/), and the primers specificity was done with genome sequences of finger millet to ensure that primers only bind to the intended target sequence. The primer sequences, annealing temperature, and product size of each primer were listed in

Table 1. Healthy and viable seeds of finger millet genotype (IC87469) was selected for this experiment, and grown under drought (15% PEG-induced drought stress) and salinity (200 mM NaCl) stress conditions according to previous protocols (Rakkammal et al., 2023b; Rakkammal et al., 2023a). Both shoot and root tissues were harvested after 28 days of growth, and they were used for gene expression analysis. Total RNA was isolated from shoot and root tissues using the Trizol method (Rakkammal et al., 2023a; Rakkammal et al., 2023b), and cDNA was synthesized using the QuantiTect Reverse transcription kit (Qiagen, Germany). *EF-1α* was

FIGURE 4
Multiple sequence alignment of *PYL* genes of finger millet, rice, and foxtail millet. MSA of putative *PYLs* genes of finger millet, rice and foxtail millets illustrate conserved GATE (CL2 loop) and LATCH (CL3 loop), essential for abscisic acid signaling.
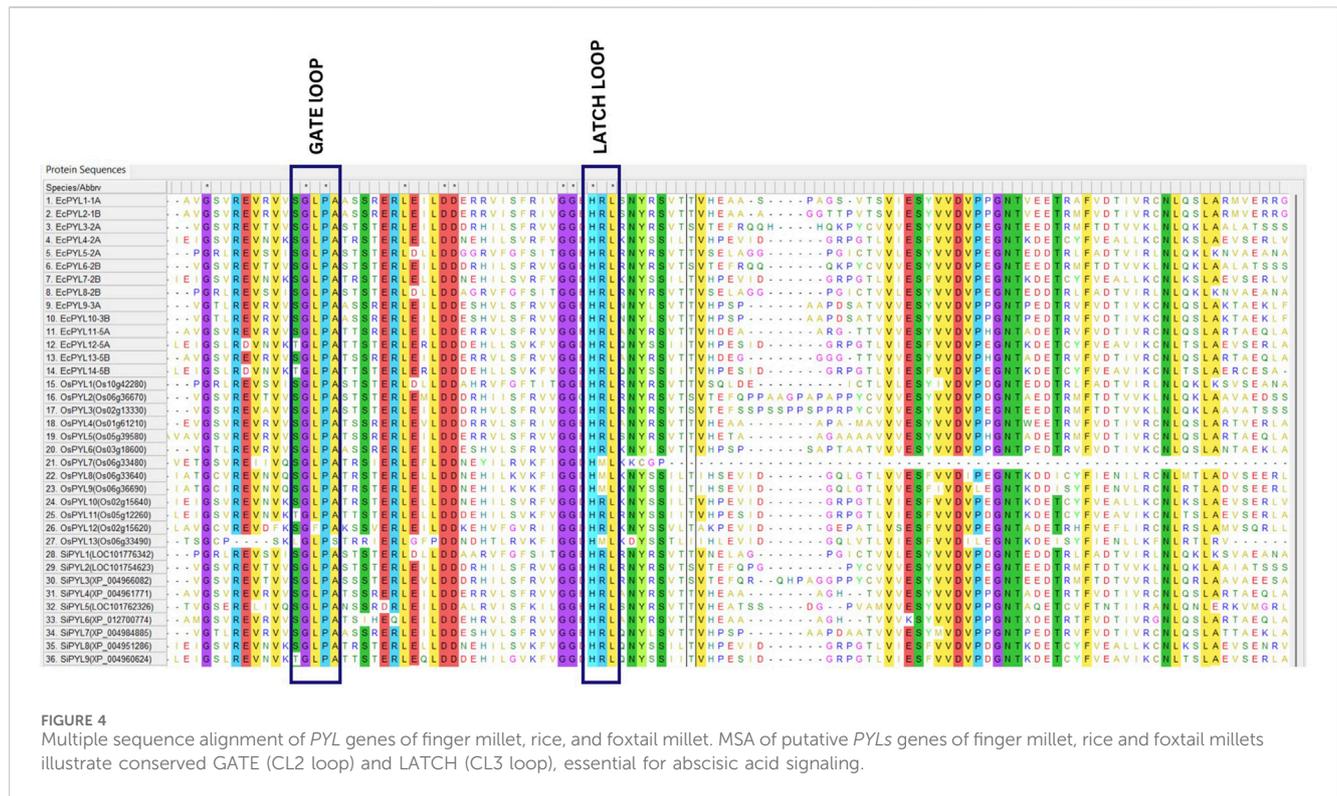
used as a reference gene to normalize the expression pattern of each *PYL* gene. Cycle threshold values of each *PYL* genes were analyzed using the formula $2^{-\Delta\Delta Ct}$. A total of three biological and three technical replicates were used for each treatment. Whereas, statistical analysis were performed through origin 2021 software (https://www.originlab.com/origin) using ANOVA, followed by Tukey test for multiple comparisons for significantly difference genes ($p \leq 0.05$).

Homology modeling of finger millet *PYLs* genes

The SWISS MODEL predicted the *in silico* structure of EcPYLs proteins (Waterhouse et al., 2018). PDBsum (http://www.ebi.ac.uk/thornton-srv/databases/pdbsum/Generate.html) and the SAVES v6.0 server (https://saves.mbi.ucla.edu/) were used to validate, analyze, and estimate the quality of the build model in two dimensions (Laskowski et al., 2018). Whereas, ResProx (http://www.resprox.ca/) (Berjanskii et al., 2012) was used to estimate the resolution of the model and SuperPose v. 1 (http://superpose.wishartlab.com/) and Biovia Discovery Studio 2019 was used for superposition and visualization of model, respectively.

Results

Sequence analysis of *PYL* genes in finger millet

A total of 27 *PYL* genes were retrieved from the finger millet genome (Supplementary Table S1). Moreover, based on

conserved domain analysis, the redundant sequences were removed, and 14 *PYL* genes were considered for further *in silico* studies. Table 2 shows the gene position, ORF length, domain position, and chromosome location of these 14 *PYL* genes. These genes have the polyketide cyclase 2/START domain and have the Pfam accession number PF10604. These 14 putative *EcPYLs* genes were unevenly distributed among four out of nine sets of chromosomes (Figure 1). The chromosomes 2A and 2B possess three *EcPYL* genes, chromosomes 5A and 5B has two *EcPYL* genes while chromosomes 1A and 1B and 3A and 3B possess only one *EcPYL* gene. *EcPYL* genes were not observed on chromosomes 4, 6, 7, 8, and 9. In general, both A and B sub-genomes have seven *EcPYL* genes, showing that there is not much difference in the number of *PYL* genes at the sub-genome level. For a better understanding, we named the possible genes *EcPYL* (*E. coracana PYL*) followed by the number of chromosomes located, for example, *EcPYL_1A*. We identified 14 *EcPYL* genes in finger millet and sequentially named them as *EcPYL1 to EcPYL14*, followed by their respective chromosomal numbers. The physicochemical attributes of putative *PYLs* of finger millet (Table 3) revealed that *EcPYLs* ranged from 181 to 222 aa. Accordingly, the molecular weight ranged from 19.5 to 23.7 kDa, and PI ranged from 5.5 to 9.3. The ORF lengths predicted by the ORF finder for *EcPYLs* ranged from 546 to 669 bp (Table 2). On the other hand, WolfsPort's predicted subcellular localization of *EcPYLs* genes revealed that the majority of the putative *PYLs* genes of finger millet were located in the cytoplasm and chloroplast (Table 3). Further, all the putative *PYLs* of finger millet were hydrophilic in nature as they possess negative value of Grand Average of Hydropathicity.
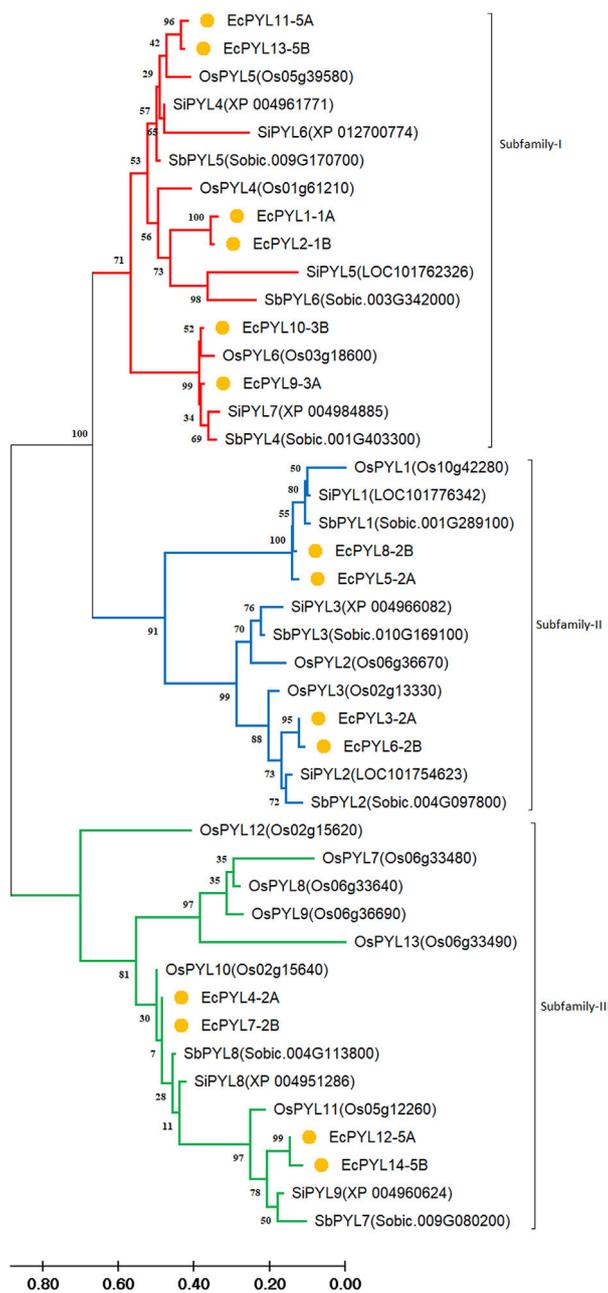
FIGURE 5
Comparative Phylogenetic analysis between finger millet, rice, foxtail millet and Sorghum. Tree was constructed by MEGA11 using Maximum Likelihood method with 1000 bootstraps Three subfamilies are represented in different colours: Subfamily-I (Red), subfamily-II (blue), and subfamily-III (Green). At the same time, the genes of finger millet throughout the phylogenetic are marked by orange nodes. The genes appear in the same clade of one subfamily having higher similarity, whereas all are evolutionarily connected. The branch length represents the magnitude of genetic change.
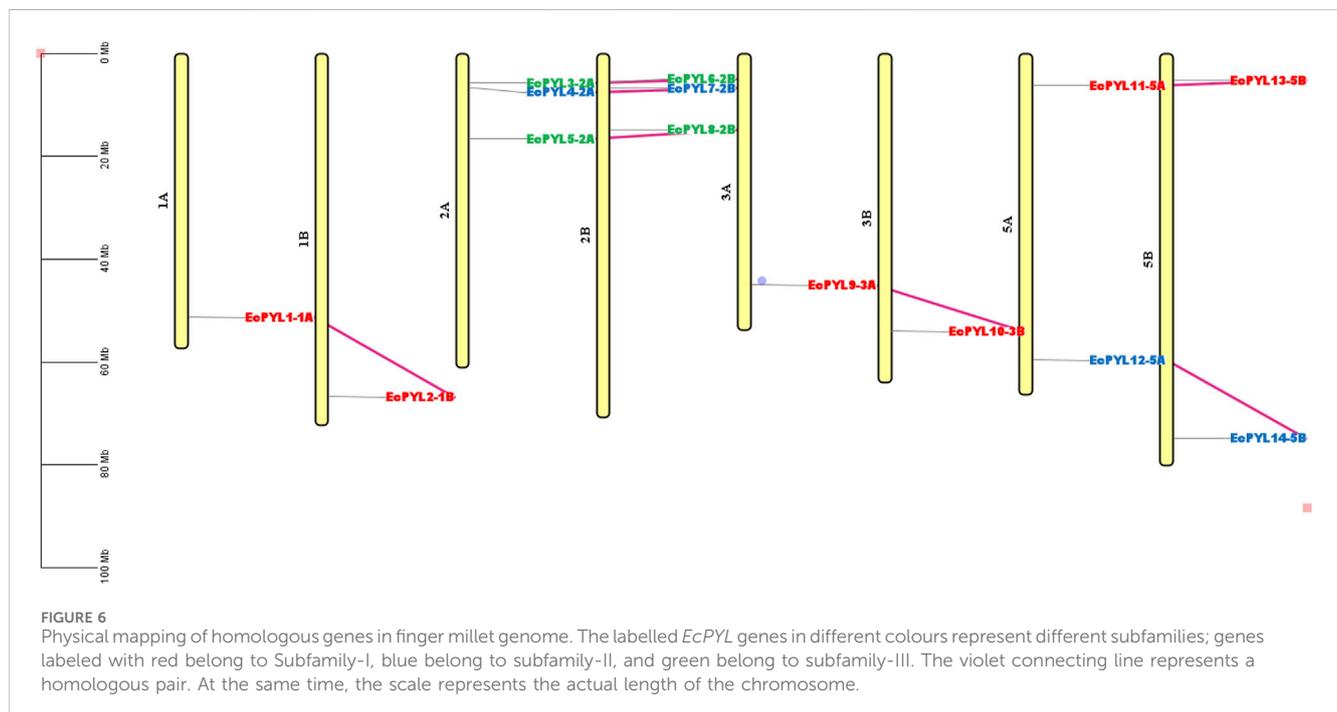
Gene structure and conserved motifs analysis

It was demonstrated that *EcPYL* can be classified into two distinct clades based on the intron/exon structure analyzed using TB tool's (Figure 2). In subfamilies I and II, no introns were detected, whereas all members of subfamily III except *EcPYL14-5B* contain two introns (Figure 2). As shown in Figure 3a, motifs 1, 2 and 3 were conserved across all *EcPYL* genes. Among the 14 *EcPYLs* studied, motif 1 contains the conserved characteristic Gate–Latch domain

(Figure 4). However, motif 4 was found to be conserved across all receptors except *EcPYL3/5/8*. Motif 5 was found to be present only in the *EcPYL3/6/9/10* genes, whereas *EcPYL11* and *EcPYL13* of the 5A and 5B chromosomes contained Motif 6. The members of the subfamily share conserved motifs and possess unique motifs (Figure 3a). The unique motifs could indicate that each member performs a unique or specialized biological function, while similar motifs reveal functional similarities. Figure 3b displays the logos of these identified motif groups, indicating the frequency of amino acid occurrence at that site.

TABLE 4 Ka vs. Ks estimation of putative *PYLs* gene of finger millet.

Gene pair	Ka	Ks	Ka/Ks ratio	Time (MYA)	Type of selection
EcPYL13-5B, EcPYL11-5A	0.009790675	0.04479112	0.2185852	3.44	Stabilizing selection
EcPYL2-1B, EcPYL1-1A	0.016148925	0.03464561	0.46611756	2.66	Stabilizing selection
EcPYL10-3B, EcPYL9-3A	0.013856485	0.05121111	0.27057576	3.93	Stabilizing selection
EcPYL6-2B, EcPYL3-2A	0.00657959	0.0474591	0.13863707	3.65	Stabilizing selection
EcPYL8-2B, EcPYL5-2A	0.01085052	0.03981233	0.2725417	3.06	Stabilizing selection
EcPYL7-2B,EcPYL4-2A	0.001426055	0.04195365	0.0339912	3.22	Stabilizing selection
EcPYL12-5A,EcPYL14-5B	0.007414455	0.02086289	0.35538964	1.60	Stabilizing selection

FIGURE 6
Physical mapping of homologous genes in finger millet genome. The labelled *EcPYL* genes in different colours represent different subfamilies; genes labeled with red belong to Subfamily-I, blue belong to subfamily-II, and green belong to subfamily-III. The violet connecting line represents a homologous pair. At the same time, the scale represents the actual length of the chromosome.
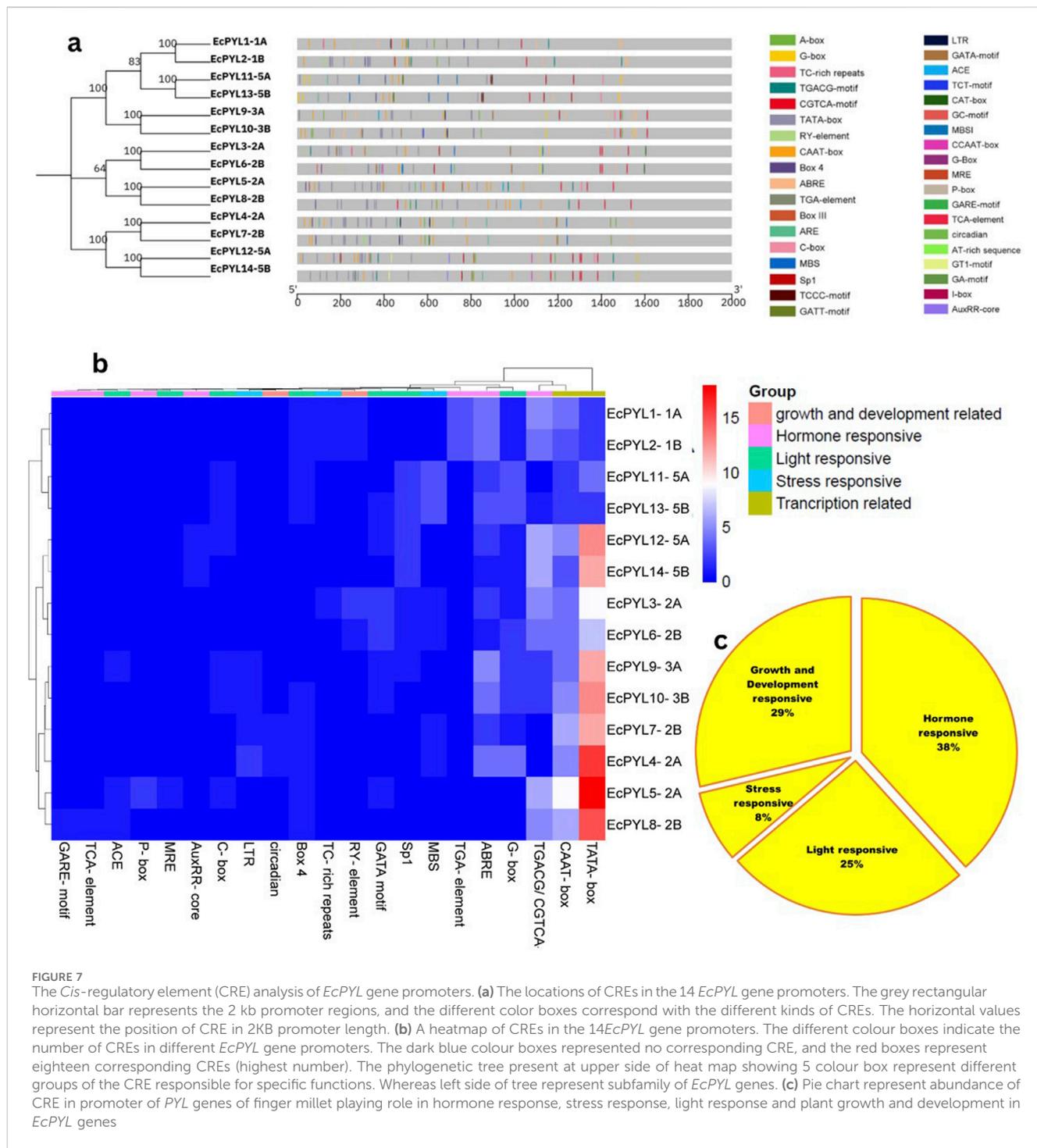
Evolutionary analysis

In terms of sequence similarity, *EcPYL* gene can be grouped in three major subfamilies, namely, subfamily-I, subfamily-II, and subfamily-III (Figure 5). Among the 14 *EcPYL* genes, *EcPYL1/2/11/13/9/10* (six *PYLs* distributed among chromosomes 1A,1B, 5A, 5B and 3A, 3B) belong to subfamily I; *EcPYL3/6/5/8* belong to subfamily II (four *PYLs* distributed among chromosomes 2A and 2B), while *EcPYL4/7/12/14* belong to subfamily III (four *PYLs* distributed among chromosomes 2A, 2B and 5A,5B). A comparative evolutionary tree (Figure 5) shows that the *PYL* genes of rice (13 *OsPYL*), sorghum (8 *SbPYL*), finger millet (9 *SiPYL*) and foxtail millet (14 *EcPYL*) are grouped together into subfamilies I, II, and III. The genes *EcPYL11/13* in subfamily I are closely related to one another and distantly related to *OsPYL5*, suggesting that these genes might be involved in signaling pathways that help plants resist the rice blast fungus (Yadav et al., 2020). Along with this, *EcPYL10* may also play a similar role because it is closely related to *OsPYL6* and has the same inhibitory phosphatase activity (Kim et al., 2014). *EcPYL9* is closely related to *SiPYL7/4* and

also has some evolutionary similarities with *EcPYL10-B* from finger millet and *OsPYL6* from rice. These evolutionary similarities are made up of conserved amino acid residues. *EcPYL3/6* belong to subfamily II of the evolutionary tree and are closely related to foxtail millet *SiPYL2* as well as to sorghum *SbPYL2*. *EcPYL4/7* are distantly related to rice *OsPYL10*, suggesting that *EcPYL4/7* could inhibit phosphatase activity without ABA (He et al., 2014). In addition, the *OsPYL7/8/9/13* appear in different subclades (Figure 5) as a result of mutations in conserved amino acid residues of the latch loop (HRL), which are replaced by HML amino acid residues (Figure 4) in the same evolutionary tree.

Non-synonymous (Ka)/synonymous (Ks) analysis

To determine the degree of selection pressure during the divergence of *PYL* genes, we evaluated the (Ka) versus (Ks) analysis for the paralogous gene pairs of finger miller PYL receptor protein. Based on the Ka versus Ks calculation tool,

FIGURE 7
The *Cis*-regulatory element (CRE) analysis of *EcPYL* gene promoters. **(a)** The locations of CREs in the 14 *EcPYL* gene promoters. The grey rectangular horizontal bar represents the 2 kb promoter regions, and the different color boxes correspond with the different kinds of CREs. The horizontal values represent the position of CRE in 2KB promoter length. **(b)** A heatmap of CREs in the 14*EcPYL* gene promoters. The different colour boxes indicate the number of CREs in different *EcPYL* gene promoters. The dark blue colour boxes represented no corresponding CRE, and the red boxes represent eighteen corresponding CREs (highest number). The phylogenetic tree present at upper side of heat map showing 5 colour box represent different groups of the CRE responsible for specific functions. Whereas left side of tree represent subfamily of *EcPYL* genes. **(c)** Pie chart represent abundance of CRE in promoter of *PYL* genes of finger millet playing role in hormone response, stress response, light response and plant growth and development in *EcPYL* genes

seven pairs of paralogous genes with their position on the chromosome were identified for finger millet PYLs proteins, as shown in Table 4 and Figure 6. The selective pressure on genes due to which encoded protein shows functional alteration can be predicted by nucleotide substitution rate, i.e., the ratio of Ka (non-synonymous) versus Ks (synonymous) (Table 4). All gene pairs with Ka/Ks < 1 indicate the possibility of synonymous substitution and stabilizing selection during evolution. Moreover, the evolutionary time study of these paralogous genes revealed that they evolved approximately 3.1 million years ago.

Cis-regulatory elements (CRE) analysis

CREs in the promoter region are known to influence transcriptional regulation greatly. Across fourteen *EcPYL* genes, 37 putative CREs were identified and mapped on the promoter
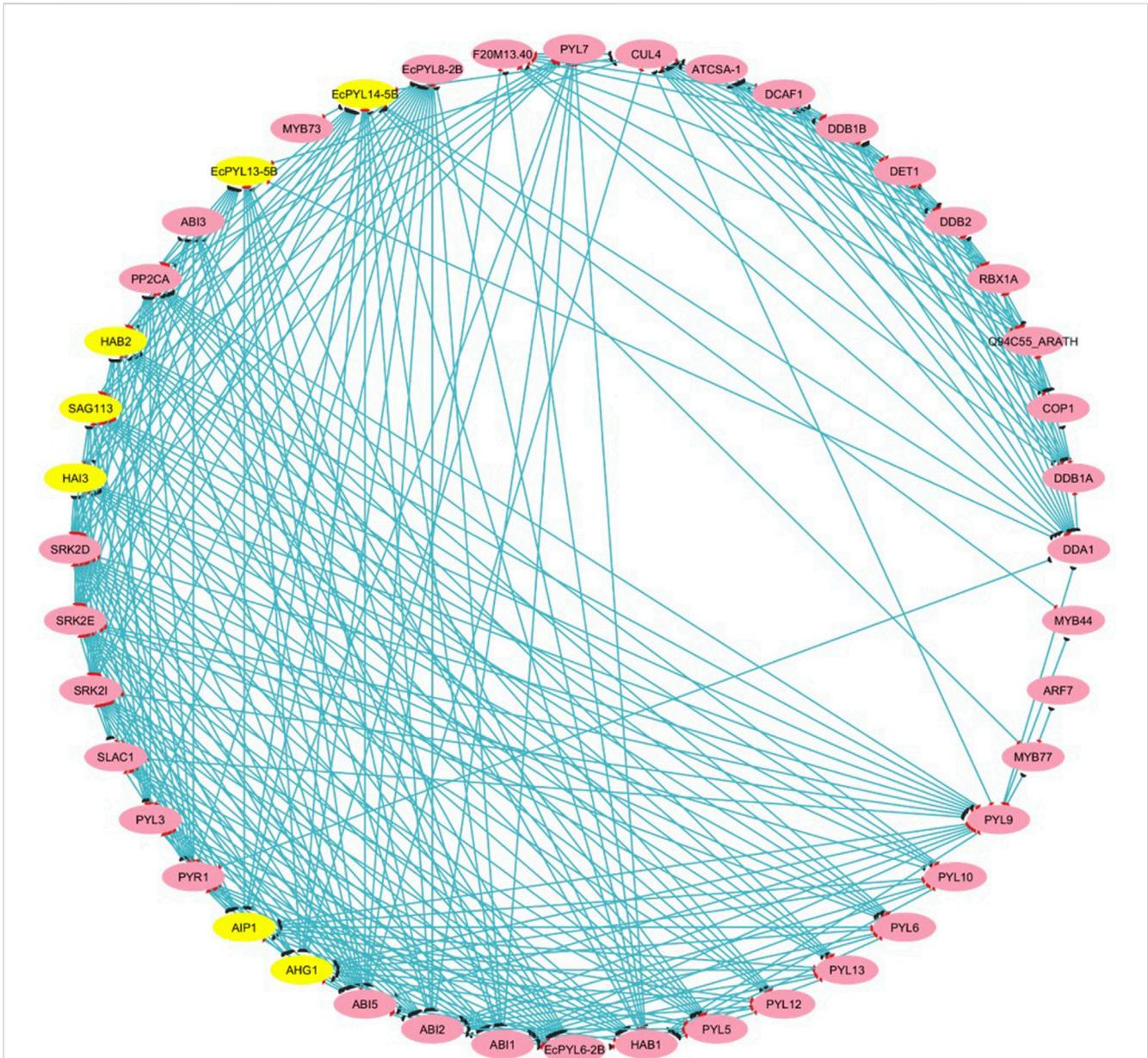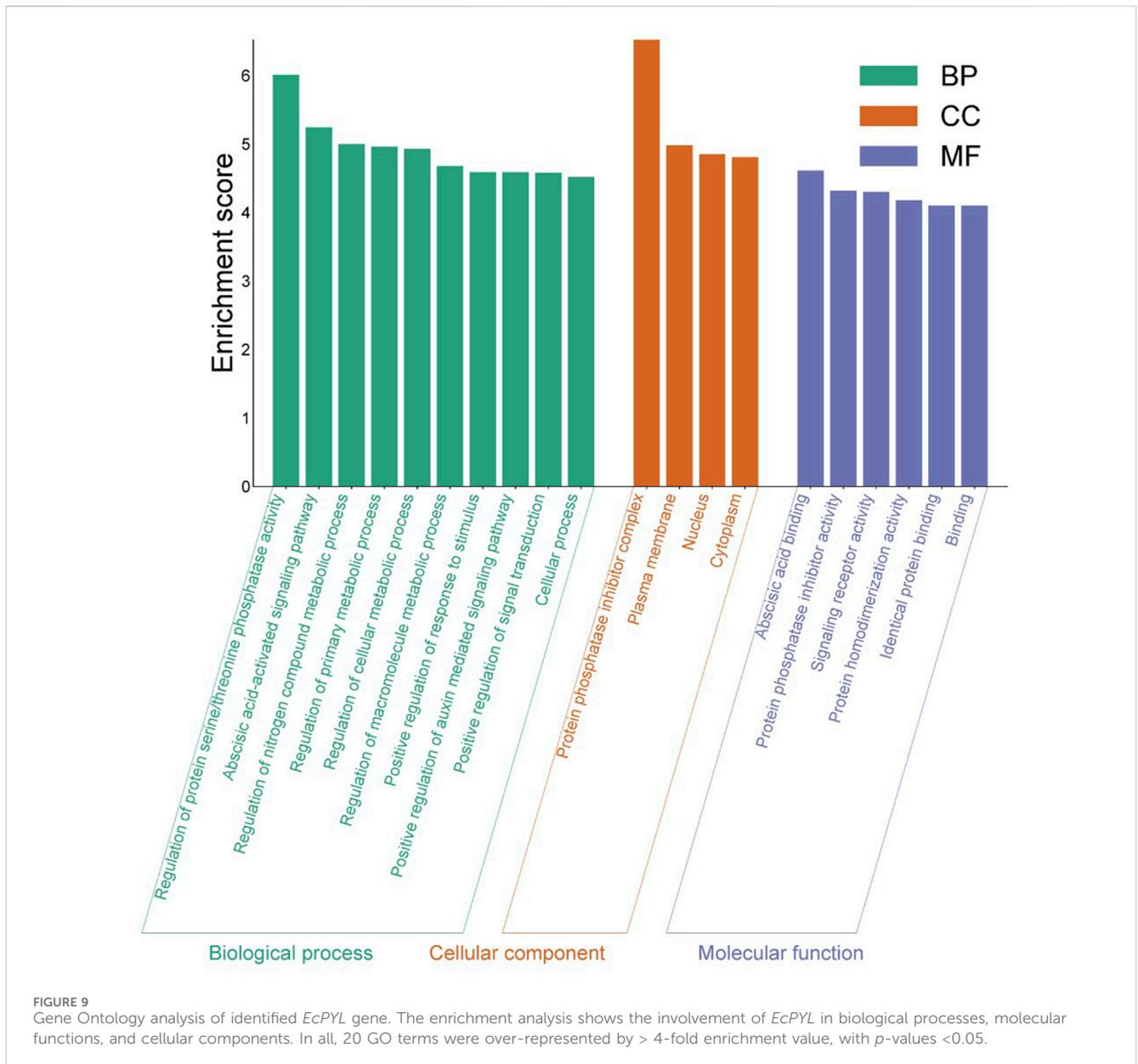
FIGURE 8
Protein-Protein (P-P) interaction analysis between putative PYLs of finger millet. The P-P interaction network is drawn using STRING tool and visualized using Cytoscape v. 3.10.3. The yellow highlights represent major genes that participated in interaction with other proteins or transcription factors that appeared in clusters analyzed through MCODE. At the same time, pink highlights represent (targets). The blue line represents the interacting string.

region of *EcPYL* genes (Figure 7a; Supplementary Table S2). Several cis-elements were found to have different functions in finger millet. These included role in hormonal signaling (ABRE, TGACG/ CGTCA-motif, P-box, GARE-motif, AuxRR-core TGA-element, and TCA-element), developmental processes (RY-element and circadian), light-responsiveness (G-box, C-box, Box 4, ACE, GATA motif MRE and Sp1) and various stresses (TC-rich repeats, LTR, MBS) in finger millet (Figure 7b). In addition to transcription-related CRE, a lot of the ABREs (abscisic acid-responsive element) and MeJA (methyl jasmonate/TGACG-motif/CGTCA-motif), which are linked to plant defense systems, were found. Furthermore, the fact that several *EcPYL* genes have

GARE (gibberellic acid-responsive elements) and ARE (auxin-responsive elements) in their promoter region suggests that hormones may interact at the level of ABA receptor expression. Among stress-responsive factors, MBS (MYB binding site involved in drought-inducibility) and LTR (low-temperature responsive elements) are commonly observed in finger millet. Further, one additional CRE has been observed to be ubiquitously present in all the *PYL* genes of finger millet, called CCAAT. This five nucleotide base motif is associated with controlling flowering in plants (Wenkel et al., 2006) and contains a binding region for Nuclear Factor-Y transcription factor (NF-Y), which has been reported to regulate several biotic and abiotic stress factors (Rani et al., 2023; Rani et al.,

FIGURE 9
Gene Ontology analysis of identified *EcPYL* gene. The enrichment analysis shows the involvement of *EcPYL* in biological processes, molecular functions, and cellular components. In all, 20 GO terms were over-represented by > 4-fold enrichment value, with *p*-values <0.05.
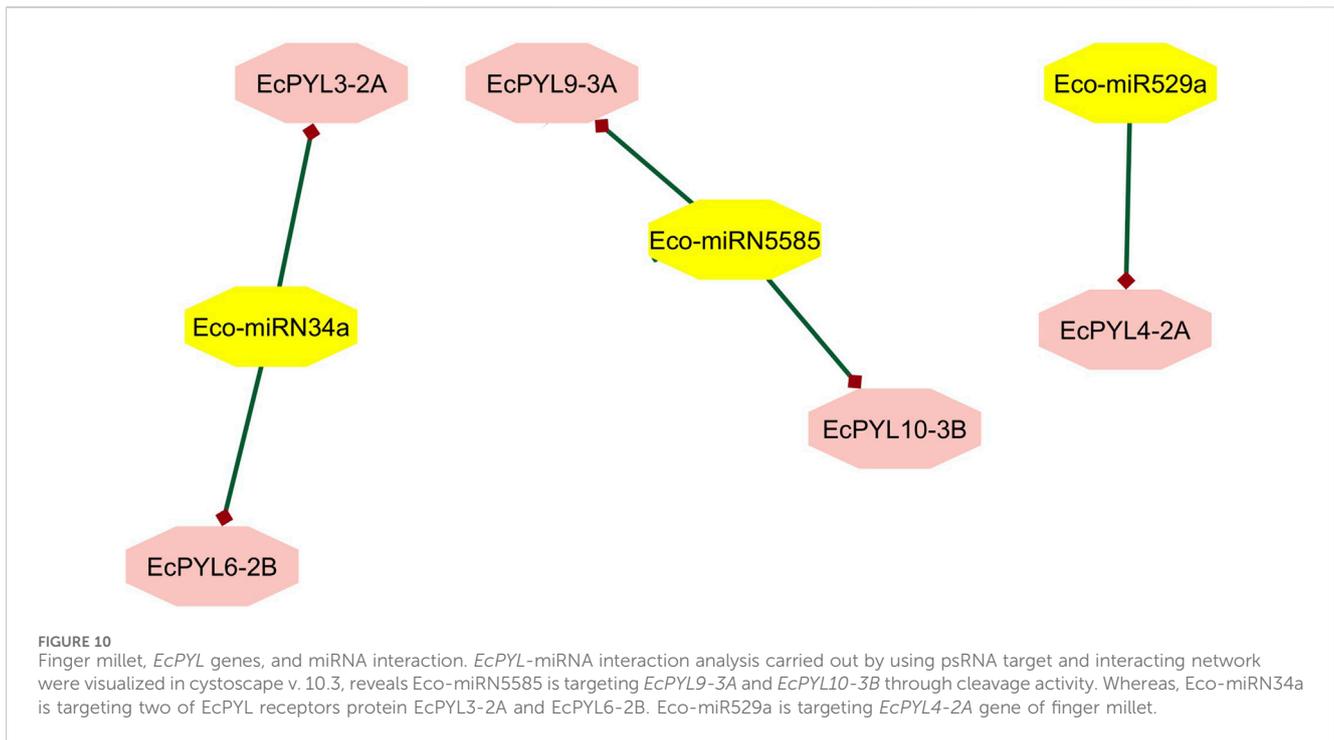
2024a; Rani et al., 2024c). Hence, the presence of different CREs (8% stress responsive, 25% light responsive, 29% growth and development related and 38% hormone responsive) in the promoter region of finger millet provides an insight into its putative role in plant development and stress tolerance (Figure 7c).

Protein-protein interaction and *EcPYL*-miRNA interaction analysis

The PPI results reveal a total of 44 nodes and 289 edges, and the MCODE of Cytoscope classifies them into three clusters. There are four *EcPYL* genes in cluster 3, and they interact with nine *Arabidopsis PYL* genes and 35 other genes performing the similar biological functions (Figure 8). In most cases, *EcPYLs* interact with PP2C, SnRK2 (the core ABA signaling complex), and the MYB transcription factor, which are vital components of the ABA-auxin

signaling complex (Figure 8). Based on functional annotation, a group of EcPYLs proteins was discovered to play a role in different biological functions (BF), molecular functions (MF), cellular component (CC) (Figure 9).

Gene ontology and enrichment analysis reveals that *EcPYL* genes are enriched in plasma membrane (GO: 0005886), nucleus (GO: 0005634), protein phosphatase inhibitor complex (GO: 0062049) in terms of cellular components. Molecular function is enriched in abscisic acid binding (GO: 0010427), protein phosphatase inhibitor activity (GO: 0004864) and signaling receptor activity (GO: 0004864). Biological processes revealed that *EcPYL* genes are involved in regulating protein serine/threonine phosphatase activity (GO: 0080163) and the abscisic acid-activated signaling pathway (GO: 0009738). Besides these functions *EcPYL* genes also involved in two KEEG pathways *viz*. mitogen-activated protein kinase (MAPK) signaling pathway (ath04016) and plant hormone signal transduction pathway (ath04075).

FIGURE 10
Finger millet, *EcPYL* genes, and miRNA interaction. *EcPYL*-miRNA interaction analysis carried out by using psRNA target and interacting network were visualized in cystoscape v. 10.3, reveals Eco-miRN5585 is targeting *EcPYL9-3A* and *EcPYL10-3B* through cleavage activity. Whereas, Eco-miRN34a is targeting two of EcPYL receptors protein EcPYL3-2A and EcPYL6-2B. Eco-miR529a is targeting *EcPYL4-2A* gene of finger millet.

In order to determine the miRNA targets and their regulation post-transcriptionally, EcPYL-miRNA interaction analysis was conducted, which revealed only three unique miRNAs targeting specific members of a particular subfamily of *PYL* genes in finger millet (Figure 10). Eco-miRN5585 targets *EcPYL9-3A* and *EcPYL10-3B* genes of subfamily I, while *Eco-miRN34a* targets *EcPYL3-2A* and *EcPYL6-2B* of subfamily-II and *Eco-miRN529a* targets only one gene *EcPYL4-2A* of subfamily III (Supplementary Table S3) through cleavage activity. Inhibition through cleavage activity appears to be the predominant mechanism by which most of the miRNAs predicted to target *EcPYL* members and regulating their expression post-transcriptionally either by positive or negative mechanism. However, miR529a were found to be involved in modulating panicle architecture in plants; however, miR5585 and miR34a were reported to play a crucial role as tumour suppressor cells (Farooqi et al., 2017). Thus, controlling *EcPYL* genes through sequence-specific interaction mediated by miRNAs could be very important for plants' ability to respond to growth and pathogen infection.
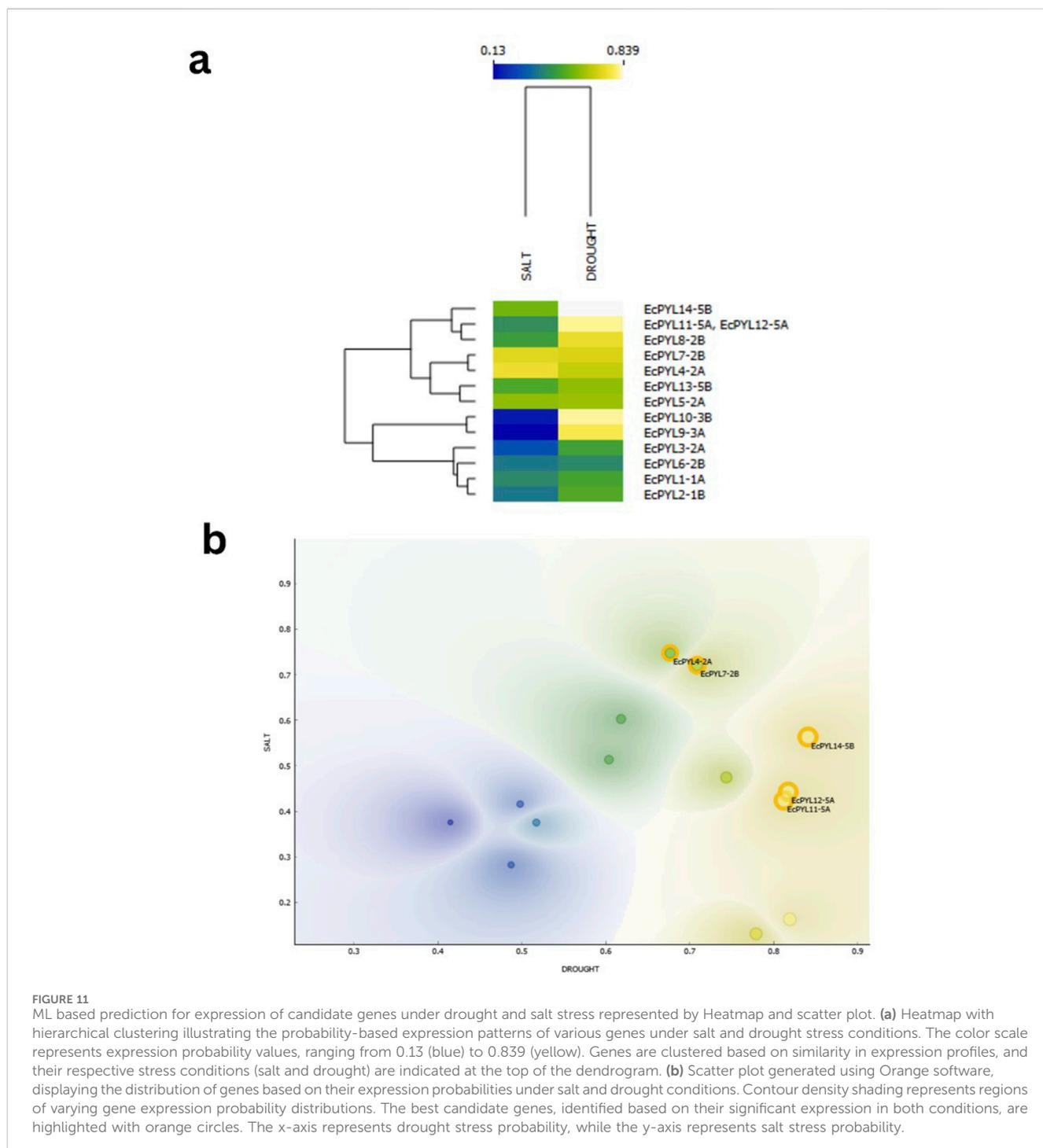
Pre-selection of candidate genes by ML algorithm

By combining scatter plot visualization (Figure 11b), hierarchical clustering (Figure 11a), and numerical probability assessments (Table 5), the expression probabilities of these genes were analyzed under both the stress conditions. Scatter plot analysis (Figure 11b) identified distinct clusters of *EcPYL* genes under salt and drought conditions, each exhibiting varying degrees of expression. *EcPYL14-5B*, *EcPYL12-5A*, *EcPYL11-5A* and *EcPYL7-2B* were most likely to be expressed during drought stress, which suggests they may be involved in mechanisms that help plants deals with drought. Conversely, *EcPYL4-2A* and *EcPYL7-2B* displayed the highest expression probabilities under salt stress (≥0.72), indicating their potential role in salinity adaptation. The hierarchical

clustering heatmap (Figure 11b), which grouped genes with similar expression patterns, further supported these observations. Drought stress strongly linked the groups of *EcPYL14-5B*, *EcPYL12-5A*, and *EcPYL11-5A*. On the other hand, *EcPYL4-2A* and *EcPYL7-2B* grouped separately, indicating their role in salinity stress. Further, *EcPYL9-3A* and *EcPYL10-3B* showed a strong preference for drought stress, while *EcPYL6-2B* exhibited a lower expression probability under both conditions. Table 5 shows that these trends were supported by the probability analysis. *EcPYL14-5B* had the highest expression probability (0.839) during drought stress, followed by *EcPYL12-5A* (0.818) and *EcPYL11-5A* (0.811). The *EcPYL4-2A* (0.749) and *EcPYL7-2B* (0.721) were also among the most highly expressed genes under salt stress. Although some genes displayed moderate expression probabilities under both stress conditions, they did not meet the threshold for high likelihood (≥0.70). For example, *EcPYL5-2A* showed a fairly balanced expression pattern (0.604 when exposed to salt and 0.618 when exposed to drought), which suggests it might play a small but important role in adapting to abiotic stress in general. However, genes such as *EcPYL9-3A* (0.13 under salt, 0.781 under drought) and *EcPYL10-3B* (0.164 under salt, 0.819 under drought) showed a distinct preference for drought-related expressions. Overall, our results show that *EcPYL14-5B*, *EcPYL12-5A*, *EcPYL11-5A* and *EcPYL7-2B* are important candidate genes and these genes are likely to be involved in regulating drought stress. While *EcPYL4-2A* and *EcPYL7-2B* are likely to regulate salinity stress.

Expression profile of *PYL* genes in finger millet under drought and salinity stress conditions

Through ML based algorithm, a total of five *PYL* genes (*EcPYL4-2A*, *EcPYL7-2B*, *EcPYL11-5A*, *EcPYL12-5A*, and

FIGURE 11
ML based prediction for expression of candidate genes under drought and salt stress represented by Heatmap and scatter plot. **(a)** Heatmap with hierarchical clustering illustrating the probability-based expression patterns of various genes under salt and drought stress conditions. The color scale represents expression probability values, ranging from 0.13 (blue) to 0.839 (yellow). Genes are clustered based on similarity in expression profiles, and their respective stress conditions (salt and drought) are indicated at the top of the dendrogram. **(b)** Scatter plot generated using Orange software, displaying the distribution of genes based on their expression probabilities under salt and drought conditions. Contour density shading represents regions of varying gene expression probability distributions. The best candidate genes, identified based on their significant expression in both conditions, are highlighted with orange circles. The x-axis represents drought stress probability, while the y-axis represents salt stress probability.

EcPYL14-5B) that respond to drought and salinity stresses were selected (Figures 11a,b), and their expression pattern was analyzed in shoot and root tissues of finger millet under drought and salinity stress (Figures 12a,b). Notably, all genes exhibited expression in both tissues under both the stress conditions (Figures 12a,b,d,f); however, their expression patterns varied between tissues and conditions (Figures 12c,e). For instance, compared to *EcPYL4-2A*, only *EcPYL12-5A* showed a 9.69-fold increase in shoot tissue under drought stress conditions (Figure 12c). When we compared the expression pattern of *EcPYL12-5A* in shoot tissue between

salinity and drought, it was observed that drought stress increased its expression level up to 2.1-fold compared to salinity stress (Fig. d–f). The expression level of *EcPYL11-5A* was higher in the shoot after *EcPYL12-5A* under drought. Under drought stress, *EcPYL7-2B* increased more than 2-fold in shoot tissue compared to *EcPYL4-2A* and *EcPYL14-5B*. Three genes (*EcPYL4-2A*, *EcPYL11-5A*, and *EcPYL14-5B*) were comparatively less active in the shoot tissue of finger millet under salt stress (Figure 12e). However, of these, *EcPYL4-2A* increased its expression level by 0.76-fold higher in shoot tissue under salinity stress than drought

TABLE 5 Probability of expression of *EcPYL* genes under salt and drought stress conditions.

Gene	Probability of expression under salt	Probability of expression under drought
EcPYL1-1A	0.415	0.497
EcPYL2-1B	0.374	0.516
EcPYL3-2A	0.282	0.486
EcPYL4-2A	0.749	0.676
EcPYL5-2A	0.604	0.618
EcPYL6-2B	0.377	0.414
EcPYL7-2B	0.721	0.808
EcPYL8-2B	0.477	0.743
EcPYL9-3A	0.13	0.781
EcPYL10-3B	0.164	0.819
EcPYL11-5A	0.422	0.811
EcPYL12-5A	0.444	0.818
EcPYL13-5B	0.512	0.603
EcPYL14-5B	0.564	0.839

The table presents the predicted probability scores for the expression of *EcPYL* genes in response to salt and drought stress, as determined by the ASRpro web server. Genes with a probability score of ≥0.70 were highly likely to be expressed under the respective stress conditions.

(Figure 12f). Two genes (*EcPYL7-2B* and *EcPYL11-5A*) showed their expression level higher (>3.5-fold) in shoot tissues under salinity stress than the other three genes. In conclusion, three genes (*EcPYL7-2B*, *EcPYL11-5A*, and *EcPYL12-5A*) and two genes (*EcPYL7-2B* and *EcPYL12-5A*) were found to be highly expressed in shoot tissue of finger millet under drought and salinity stresses, respectively.

In the root, *EcPYL2-7B* exhibited highest expression among the five PYLs under both stresses. Notably, expression level of *EcPYL12-7B* increased by more than 15-fold compared to *EcPYL11-5A*, *EcPYL12-5A*, and *EcPYL14-5B* under salinity stress. Similarly, the same gene demonstrated 1.96-fold higher expression in the root under salinity stress compared to *EcPYL4-2A*. However, *EcPYL4-2A* expression was up to 9.3 times higher than *EcPYL11-5A*, 13.5 times higher than *EcPYL12-5A*, and 17.6 times higher than *EcPYL14-5B* in the root under salinity stress. Interestingly, the expression levels of the same three genes—*EcPYL11-5A*, *EcPYL12-5A*, and *EcPYL14-5B* was enhanced by 6.15, 12.26, and 4.6 times in root tissues under drought stress. Moreover, *EcPYL7-2B* alone had highest expression in the root under drought stress among the five genes. For instance, the expression level of this gene was almost 1.5 times higher than that of the other genes. Overall, *EcPYL4-2A* and *EcPYL7-2B* showed higher expression in the root tissue, under both the stress conditions suggesting that *EcPYL7-2B* is the most responsive gene under drought and salinity stress, particularly in root tissues, while *EcPYL12-5A* and *EcPYL11-5A* play significant roles in shoot tissues under drought stress. This differential expression highlights the potential role of these genes in stress adaptation and provides insights for future functional studies on drought and salinity tolerance mechanisms in finger millet.

Homology modeling of finger millet *PYLs* genes

Protein sequences, EcPYL13-5B, EcPYL6-2B, EcPYL8-2B, and EcPYL14-5B representing each clade of the phylogenetic tree, were used for homology modeling for structural prediction (Figure 5). The widely preferred method for modeling protein structures is to compare a sequence of our interest, i.e., the target sequence (unknown structure), with a template (known structure) and look for structural similarities. The SWISS-MODEL server (https://swissmodel.expasy.org/) was used in the present study for homology modeling of *EcPYL6-2B, EcPYL8-2B, EcPYL13-5B,* and *EcPYL14-5B* (Figure 13) against best-matched template 4oic, 5ujv and 5gwo, respectively, based on the high percent of identity, as shown in Table 5. The model generated by these templates was further validated by the SAVES server by analyzing the number of amino acid residues in allowed or disallowed areas through PROCHECK, accuracy of non-bonded contact by ERRAT (Table 6). All the models had ERRAT scores greater than the acceptable value of 80%. After the accuracy measurement, the modeled structure was subjected to the degree of similarity search with the crystal structure of (PDB ID 4oic, 5ujv and 5gwo) by using SuperPose V.1. The RMSD (Root Mean Square Deviation) and NRES (Number of Overlapped Residue) were analyzed for the superposed structure as shown in Table 4. By evaluating the result of the superposition, it can be concluded that the quality of the model is good, with the least deviation of residues from the template. Further, validation of the predicted model was performed with ResProx resolution criteria (Good: 0–1.5, Middle: 1.5–2.5, Bad: >2.5), indicating the models to be of good resolution. Table 6 summarizes the detailed analysis of homology modeling using SWISS-MODEL, structural assessment, SAVES server
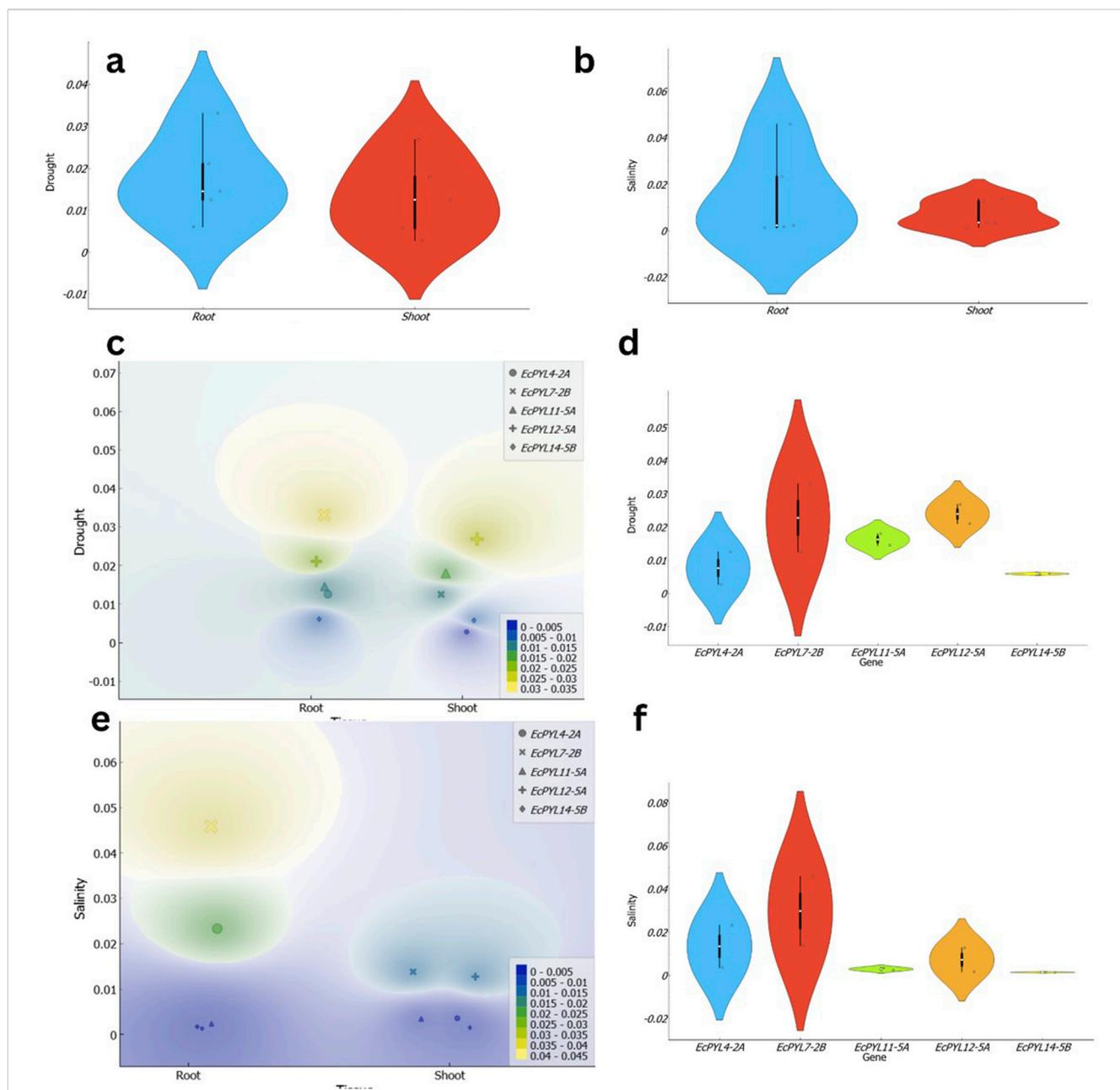
FIGURE 12
Illustration of the expression patterns of *EcPYL* genes in finger millet under drought and salinity stress across shoot and root tissues. **(a,b)** present violin plots depicting the distribution of *EcPYL* gene expression under drought and salinity stress, respectively. In **(a)**, the expression levels under drought conditions exhibit a broader distribution in root tissues (blue) compared to shoot tissues (red), suggesting higher variability in root responses. Similarly, in **(b)**, under salinity stress, root tissues display a wider expression range than shoot tissues, as indicated by the distribution density and black boxplots representing the median, interquartile range, and data spread. **(c,e)** depict density-based expression heatmaps of *EcPYL* genes under drought and salinity stress, respectively. In **(c)**, the density plot illustrates the spatial expression distribution of *EcPYL4-2A, EcPYL7-2B, EcPYL11-5A, EcPYL12-5A*, and *EcPYL14-5B* across root and shoot tissues under drought stress. The color gradient represents expression density, where yellow and green indicate high expression levels, while blue represents low expression levels. A similar pattern is observed in **(e)** under salinity stress, where root tissues exhibit a more pronounced variation in expression, while shoot tissues display a more localized expression response. **(d,f)** show violin plots representing the expression profiles of individual *EcPYL* genes under drought and salinity stress, respectively. Under drought stress **(d)**, *EcPYL7-2B* exhibits the highest variation, while *EcPYL14-5B* remains relatively stable across both tissues. Similarly, under salinity stress **(f)**, *EcPYL7-2B* again shows the highest expression variability, whereas *EcPYL11-5A* and *EcPYL14-5B* demonstrate limited fluctuations in expression levels.

validation, and quality and resolution estimation using SuperPOSE v.1 and ResProx. The 2-D structural analysis performed by the PDBSum server revealed that finger millet *EcPYLs* genes (*EcPYL6-2B, EcPYL8-2B, EcPYL13-5B*, and *EcPYL14-5B*) contains same number of strand but having different number of helices as 5:4:5:4 respectively (Table 6). Figure 13 depicts each model's conserved residues present in CL2 (GATE loop) and CL3 (LATCH loop), specific for ABA binding.
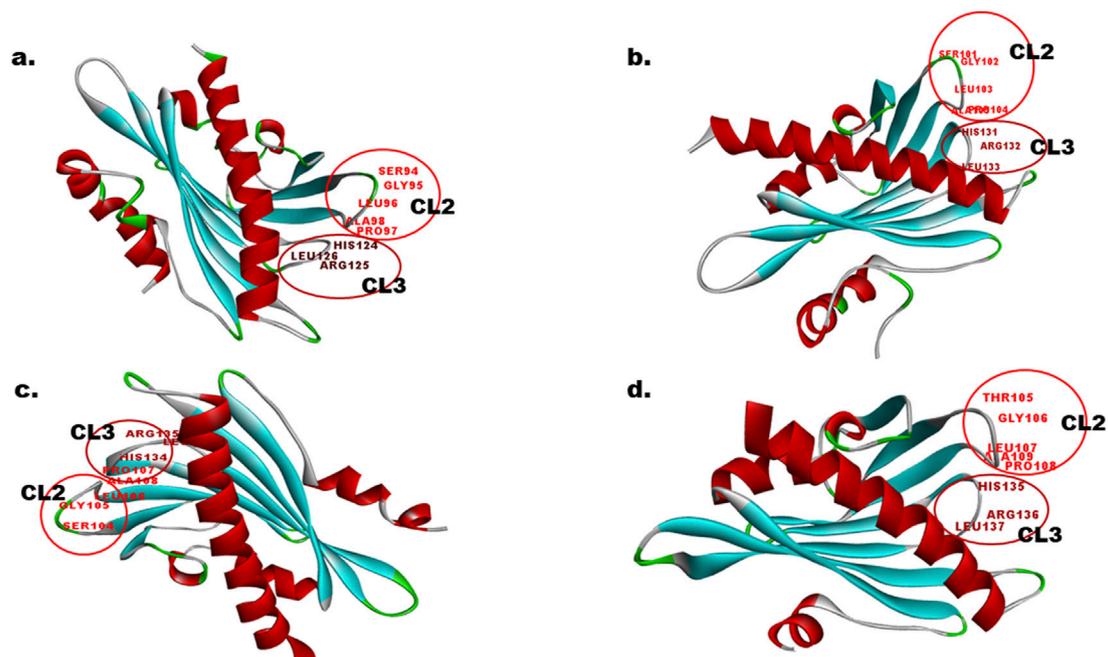
FIGURE 13
In-silico structural analysis of EcPYL proteins. The 3D structure modeling of EcPYL proteins was generated using the SWISS-MODEL and visualized by Biovia Discovery Studio. The alpha helix is represented by red colour, beta-sheets by cyan colour, coil by green and loops by gray colour. The conserved amino acids residue represented on loop (CL2 and CL3 loop) with their position, participating in ABA signaling **(a)** EcPYL6-2B, **(b)** EcPYL8-2B, **(c)** EcPYL13-5B, and **(d)** EcPYL14-5B.

Discussion

The *PYL* gene family is found in a variety of plant species, including *Arabidopsis* (Gonzalez-Guzman et al., 2012), rice (Kim et al., 2012; Yadav et al., 2020), sorghum (Dalal and Inupakutika, 2014), maize (Fan et al., 2018; Wang et al., 2018) and wheat (Lei et al., 2021). Rani et al. (2024c) reported three *EcPYL* genes (GJN19492.1, GJN35776.1, GJN19381.1) in finger millet based on rice homologs. However, the in-depth characterization and molecular validation of PYL receptors is yet to be explored in finger millet. A total of 14 *EcPYL* genes were identified in finger millet in the present study, which are distributed into three subfamilies designated as subfamily I, II and III respectively. Evolutionary analysis coupled with MEME search revealed a diversity of conserved motifs in finger millet and other cereals *PYL* genes. Whereas, the gene structure analysis showed presence of a common exon or intron structure in most of the genes within a subfamily. The members of *EcPYLs* in Subfamilies I and II are intronless and have conserved motifs 1, 2, and 3. However, only Subfamily III members contain introns and are conserved for motifs 1, 2, 3 and 4. Whereas motif 5 was observed among members of subfamily 2, and motif 6 was found only among two members of subfamily I. *EcPYL* genes in the same subfamily have gradually developed different protein motif structures due to adaptation to complex environmental conditions during the evolution of the finger millet genome. As compared to 14 *PYLs* in finger millet, there exist 13 *PYLs* in rice (Yadav et al., 2020), 8 *PYLs* in sorghum (Dalal and Inupakutika, 2014) and 9 *PYLs* in foxtail millet (Wu et al., 2023). The *EcPYLs* revealed close genetic proximity with rice and

divergence with sorghum and foxtail millet *PYLs*. The variability could be attributed to gene duplication events resulting from polyploidization, which contribute to gene family expansion and genome evolution (Moore and Purugganan, 2005).

The chromosomal location of these *EcPYL* genes were determined and it was found that it exists as seven pairs of homologous genes present on homologous chromosomes 1, 2, 3, and 5. Most of these genes are located on chromosomes 2A and 2B. As a result of genome polyploidization, some homologous genes might have lost (Lynch and Force, 2000). Gene duplication plays an important role in expanding the *PYL* gene family with possibility for new biological functions (Conant and Wolfe, 2008). The analysis of cis-regulatory elements indicated that *EcPYLs* is associated with diverse roles such as hormone-responsive, light-responsive, stress-responsive, growth, development-responsive, and transcription-responsive genes. It has been reported that over-expression of *PYL* genes in *Arabidopsis* enhances the plant's sensitivity to ABA during seed germination, growth, stomata regulation, and drought tolerance (Ma et al., 2009). Moreover, Rice ABA receptor OsPYL5 regulates ABA signaling, thereby improving drought and salinity tolerance and ABA sensitivity during germination and seedling development (Kim et al., 2012; Kim et al., 2014). Based on this analysis, it is evident that *PYL* genes may regulate finger millet growth and development and are actively involved in stress responses. Additionally, the presence of CCAAT cis-acting element in its promoter region indicates its involvement in regulation of flowering and providing binding site for nuclear factor-Y (NF-Y) transcription factor (Wenkel et al., 2006; Muthamilarasan et al., 2014; Rani et al., 2023). Further, this NF-Y-PYL/PYR module could regulate the

TABLE 6 Homology modelling, assessment, and validation of putative *EcPYLs* gene of finger millet, participated in Protein-Protein interaction.

Homology modeling				Structural assessment and validation				
Genes	Template PDB ID	Identity	Q MEAN D	Residues in most favoured regions	Residues in additional allowed regions	Residues in generously allowed regions	Residues in disallowed regions	ERRAT
EcPYL6-2B	4oic.1.A	77.72%	0.87 ± 0.06	92%	6.70%	1.20%	0.00%	81.6
EcPYL8-2B	5ujv.1.A	83.68%	0.87 ± 0.06	95%	4.90%	0	0	82.69
EcPYL13-5B	5ujv.1.A	55.56%	0.72 ± 0.07	95%	4.90%	0	0	84.67
EcPYL14-5B	5gwo.1.B	78.40%	0.86 ± 0.07	88.90%	11.10%	0	0	87.4

Quality and resolution estimation				2-Dimensional structural analysis						
Template resolution	Resolution of predicted model	RMSD	NRES	Helix	Strand	Beta turn	Beta hairpins	Helix-helix interacs	Gamma turn	Beta bulges
2.1	1.5	0.64	0.9	5	7	13	5	3	2	6
1.3	1.1	0.5	0.51	4	7	14	5	1	1	7
1.3	1.3	1.53	1.32	5	7	12	5	2	1	5
2	1.3	0.38	0.35	4	7	12	5	1	2	4

expression of the ABA receptor and enhance ABA signal transduction via transcriptional regulation of PYR1 (Yu et al., 2021). This, in turn, promotes the expression of stress-responsive genes against drought and salt stress (Yu et al., 2021). Finger millet, extremely tolerant to drought and salt (Gupta et al., 2017; Antony Ceasar et al., 2018; Sood et al., 2019; Ceasar, 2022; Rani et al., 2023), possesses fourteen *PYLs* genes and shows an interaction network with several TFs (Figure 8). ABA has been found to play a crucial role in responding to abiotic stresses such as drought and salinity and ABA signaling is initiated by PYLs (Rani et al., 2024c). Many plants have been reported to have differential expression patterns of *PYL* genes within their tissues. Soybean seeds express many *PYL* genes at a relatively high level compared to other soybean tissues (Bai et al., 2013). The rubber tree, the transcript abundance of *PYL* genes is high in latex (Guo et al., 2017). Similarly, in rice *PYLs* genes are expressed at higher levels in root tissue under drought stress than in other tissues (Yadav et al., 2020). Under drought and salinity stress, finger millet exhibits a significant ABA response, but specific PYL responsible for this is still not deciphered. In the present study, *EcPYL7-2B* demonstrated their role in regulating both drought and salinity stress. Moreover, some of the genes like *EcPYL14-5B* of finger millet were found to be comparatively less expressed as compared to other genes under drought and salinity stress, which is in accordance with previous studies reported in sorghum, rice, grapes and tomato (Boneh et al., 2012; González-Guzmán et al., 2014; Yadav et al., 2020). This behavior may be explained by a negative feedback regulatory mechanism which indicates that when excessive amounts of ABA accumulate in leaves under stress, PYL expression may be inhibited (Merlot et al., 2001; Santiago et al., 2009) or the function of these genes may not be required for drought and salinity stress (Di et al., 2018). Based on the expression profiling results coupled with stress-responsive cis-elements in *EcPYL* promoters, it appears that some *EcPYLs* are responsive to drought and salinity. Hence, these PYLs may be potential candidate to enhance finger millet tolerance to abiotic stress.

An extensive network of interactions between PYL proteins of finger millet and *Arabidopsis* genes has been predicted. As a major component of the ABA signaling pathway, PYL interacts with SnRK and PP2C in finger millet (Figure 8). PP2CA inhibits ABA metabolism, essential to seed germination and cold tolerance (Romero et al., 2012). In guard cells that recognize ABA, ABI1 modulates both calcium channel permeability and actin reorganization within stomatal closure (Tähtiharju et al., 2002). It has been found that several finger millet *PYL* genes interact with PP2CA and ABI1, suggesting its possible role in seed germination and vernalization. In response to auxin stimulation, PYL8-MYB77 interaction enhances transcription activation of IAA19 in *Arabidopsis* (Shin et al., 2007). Similarly, it was observed that *EcPYL14-5B* interacts with MYB77 (Shin et al., 2007) and MYB44 (Qin et al., 2022), indicating that both proteins participate in ABA-auxin signaling and show multiple stress tolerance. Further, to decipher the relation between ABA signaling and miRNA regulation, a PYLs-miRNA interaction study was performed. The interaction between PYLs and miRNA reveals that *miRNA5585* targets *EcPYL10-3B* and *EcPYL9-3A*, while *miRNA34a* targets *EcPYL3-2A* and *EcPYL6-2B,* as shown in Supplementary Table S3. In contrast, *EcPYL4-2A* was targeted by *miRNA529a*, suggesting that *EcPYL4-2A* are involved in a complex regulatory network and might be associated with the panicle architecture (Yue et al., 2017). The protein interaction networks

and miRNA-mediated pathways of *PYLs* genes elucidated in the present study might reveal a better understanding of the ABA signal transduction pathway in finger millet.

The structural studies attempted revealed that PYR/PYL belong to the Bet v superfamily, which contains the Bet v fold or START/polypeptide cyclase2 domain (Radauer et al., 2008). A beta-sheet with seven strands flanked by two alpha helices is referred to as a helix-grip fold. As an additional characteristic of this family of ABA receptors, the PYR/PYL family contains an alpha helical segment at their N-terminus, which is not found in the Bet v fold. Therefore, this segment can be considered as a typical characteristic of this family of ABA receptors (Santiago et al., 2012). Based on the crystallographic structure analysis of *Arabidopsis PYL* genes, it is evident that this gene contains a seven-stranded beta-sheet flanked by two alpha-helices (α1 and α2) and an additional alpha-helical segment (α0) at its N terminus. These alpha helices and beta sheets are connected with four conserved loops: CL1 connecting (α1 and β2), CL 2 connecting (β3 and β4), CL3 connecting (β5 and β6), and CL4 connecting (β7 and α2) (Yin et al., 2009). The *in silico* homology modeling attempted for the four PYLs of finger millet *EcPYL6-2B, EcPYL8-2B, EcPYL13-5B,* and *EcPYL14-5B* revealed seven strands flanking with two alpha helices with the presence of additional alpha helices at N-terminal. This indicates ABA receptor family having START domain. As shown in Figure 9, the helices and strands possess conserved CL1, CL2, CL3 and CL4. As reported for *Arabidopsis* crystal structure (PDB ID 4oic, 5ujv and 5gwo), the CL2 loop are conserved for Ser(S), Gly(G), Leu (L), Pro(P), Ala(A) amino acid residues whereas, CL3 loops are conserved for His (H), Arg (R) and Leu (L) amino acid residue (Yin et al., 2009). The constructed models of *EcPYL* showed conserved amino acids in the CL2 and CL3 loops (Figure 9), except *EcPYL14-5B*, where Ser (S) gets replaced by Thr (T) at the CL2 loop. Similar substitution has also been observed in maize *PYL* genes, which contain a conserved GATE loop or CL2 loop (SGLPA replaced with TGLPA amino acid residue) (Wang et al., 2018; Yadav et al., 2020). Hence, *PYL* genes in finger millet possess a conserved CL2 loop, which plays a vital role in ABA binding (Yin et al., 2009) and provides valuable information regarding their biological function. In order to achieve a high standard of quality, the model should contain over 90% of the residues in the most allowed regions (Laskowski et al., 2018). The model structure of this study indicates that 92%–95% of residues are mostly in allowed regions (Supplementary Figures S1–S4; Table 5), indicating that the predicted models can be accepted. The predicted structural insights provide an opportunity for deciphering the putative functions of EcPYL receptors in finger millets, which could be explored for crop improvement after validation through extensive wet-lab based experimentations.

Conclusion

Finger millet genome mining for deciphering the putative *PYL* genes has been attempted in the present study. A total of 14 identified *EcPYL* genes have been extensively characterized *in silico* for multiple structural and functional properties.

Chromosomal location, exon-intron structure, motif evaluation, and cis-regulatory element analysis and evolutionary analysis have been performed, revealing that the *EcPYLs* gene of finger millet is structurally and evolutionarily conserved among the three subfamilies. The presence of various cis-regulatory elements in the *EcPYLs* of finger millet may be involved in the enhancement of various stresses and developmental processes. Five genes (*EcPYL4-2A, EcPYL7-2B, EcPYL11-5A, EcPYL12-5A* and *EcPYL145B*) were found to be respond to drought and salinity stresses through machine learning approaches. Gene expression analysis revealed that under salinity and drought stress conditions, two key genes *EcPYL7-2B* and *EcPYL12-5A* were highly induced in shoot and root tissues. Further targeting of these two genes by genome editing approaches will help to identify the exact role of these genes in finger millet, which will aid in further breeding program. In addition, several CREs were found in this study from the promoter regions of *EcPYLs* of finger millet. Targeting drought and salinity stress responsive CREs using CRISPR activators has the potential to influence the expression of the downregulated *EcPYLs* genes. These significant findings could be applied for crop improvement programs by providing an insight into ABA signaling pathways associated with stress tolerance mechanisms in finger millet.

Data availability statement

The datasets presented in this study can be found in online repositories. The names of the repository/repositories and accession number(s) can be found in the article/Supplementary Material.

Author contributions

VR: Visualization, Writing – original draft, Formal Analysis, Methodology, Investigation, Software, Data curation, Validation, Writing – review and editing, Conceptualization. TM: Validation, Methodology, Writing – review and editing, Formal Analysis, Software. SS: Data curation, Methodology, Writing – review and editing. DJ: Resources, Writing – review and editing. RG: Writing – review and editing. DY: Data curation, Writing – review and editing, Investigation, Supervision, Funding acquisition, Formal Analysis.

Funding

References

Antony Ceasar, S., Maharajan, T., Ajeesh Krishna, T. P., Ramakrishnan, M., Victor Roch, G., Satish, L., et al. (2018). Finger millet [*Eleusine coracana* (L.) Gaertn.] improvement: current status and future interventions of whole genome sequence. *Front. Plant Sci.* 9, 1054. doi:10.3389/fpls.2018.01054

Acknowledgments

Conflict of interest

The authors declare that the research was conducted in the absence of any commercial or financial relationships that could be construed as a potential conflict of interest.

Generative AI statement

The author(s) declare that no Generative AI was used in the creation of this manuscript.

Publisher's note

All claims expressed in this article are solely those of the authors and do not necessarily represent those of their affiliated organizations, or those of the publisher, the editors and the reviewers. Any product that may be evaluated in this article, or claim that may be made by its manufacturer, is not guaranteed or endorsed by the publisher.

Supplementary material

The Supplementary Material for this article can be found online at: https://www.frontiersin.org/articles/10.3389/fgene.2025.1598523/full#supplementary-material

SUPPLEMENTARY FIGURE S1
PROCHECK analysis of EcPYL6-2B.

SUPPLEMENTARY FIGURE S2
PROCHECK analysis of EcPYL8-2B.

SUPPLEMENTARY FIGURE S3
PROCHECK analysis of EcPYL13-5B.

SUPPLEMENTARY FIGURE S4
PROCHECK analysis of EcPYL14-5B.

SUPPLEMENTARY TABLE S1
Retrieved PYL protein sequence (27) after BLASTP search against phytozome database in Finger millet genome.

SUPPLEMENTARY TABLE S2
Cis regulatory elements in promoter region of *EcPYLs* genes.

SUPPLEMENTARY TABLE S3
Putative miRNA and their targeted *PYLs* genes in finger millet.

Bader, G. D., and Hogue, C. W. V. (2003). An automated method for finding molecular complexes in large protein interaction networks. *BMC Bioinforma.* 4, 2. doi:10.1186/1471-2105-4-2

Bai, G., Yang, D.-H., Zhao, Y., Ha, S., Yang, F., Ma, J., et al. (2013). Interactions between soybean ABA receptors and type 2C protein phosphatases. *Plant Mol. Biol.* 83, 651–664. doi:10.1007/s11103-013-0114-4

Bailey, T. L., Johnson, J., Grant, C. E., and Noble, W. S. (2015). The MEME suite. *Nucleic Acids Res.* 43, W39–W49. doi:10.1093/nar/gkv416

Berjanskii, M., Zhou, J., Liang, Y., Lin, G., and Wishart, D. S. (2012). Resolution-by-proxy: a simple measure for assessing and comparing the overall quality of NMR protein structures. *J. Biomol. NMR* 53, 167–180. doi:10.1007/s10858-012-9637-2

Boneh, U., Biton, I., Zheng, C., Schwartz, A., and Ben-Ari, G. (2012). Characterization of potential ABA receptors in Vitis vinifera. *Plant Cell Rep.* 31, 311–321. doi:10.1007/s00299-011-1166-z

Ceasar, S. A. (2022). The role of millets in attaining United Nation's sustainable developmental goals. 345–349. doi:10.1002/ppp3.10254

Chao, J., Li, Z., Sun, Y., Aluko, O. O., Wu, X., Wang, Q., et al. (2021). MG2C: a user-friendly online tool for drawing genetic maps. *Mol. Hortic.* 1–4, 16. doi:10.1186/s43897-021-00020-x

Chen, C., Chen, H., Zhang, Y., Thomas, H. R., Frank, M. H., He, Y., et al. (2020). TBtools: an integrative toolkit developed for interactive analyses of big biological data. *Mol. Plant* 13, 1194–1202. doi:10.1016/j.molp.2020.06.009

Cheng, C.-Y., Krishnakumar, V., Chan, A. P., Thibaud-Nissen, F., Schobel, S., and Town, C. D. (2017). Araport11: a complete reannotation of the *Arabidopsis thaliana* reference genome. *Plant J.* 89, 789–804. doi:10.1111/tpj.13415

Conant, G. C., and Wolfe, K. H. (2008). Turning a hobby into a job: how duplicated genes find new functions. *Nat. Rev. Genet.* 9, 938–950. doi:10.1038/nrg2482

Cutler, S. R., Rodriguez, P. L., Finkelstein, R. R., and Abrams, S. R. (2010). Abscisic acid: emergence of a core signaling network. *Annu. Rev. Plant Biol.* 61, 651–679. doi:10.1146/annurev-arplant-042809-112122

Dai, X., and Zhao, P. X. (2011). psRNATarget: a plant small RNA target analysis server. *Nucleic Acids Res.* 39, W155–W159. doi:10.1093/nar/gkr319

Dalal, M., and Inupakutika, M. (2014). Transcriptional regulation of ABA core signaling component genes in sorghum (*Sorghum bicolor* L. Moench). *Mol. Breed.* 34, 1517–1525. doi:10.1007/s11032-014-0114-3

Devos, K. M., Qi, P., Bahri, B. A., Gimode, D. M., Jenike, K., Manthi, S. J., et al. (2023). Genome analyses reveal population structure and a purple stigma color gene candidate in finger millet. *Nat. Commun.* 14, 3694. doi:10.1038/s41467-023-38915-6

Di, F., Jian, H., Wang, T., Chen, X., Ding, Y., Du, H., et al. (2018). Genome-wide analysis of the PYL gene family and identification of PYL genes that respond to abiotic stress in Brassica napus. *Genes (Basel)* 9, 156. doi:10.3390/genes9030156

Duarte, K. E., de Souza, W. R., Santiago, T. R., Sampaio, B. L., Ribeiro, A. P., Cotta, M. G., et al. (2019). Identification and characterization of core abscisic acid (ABA) signaling components and their gene expression profile in response to abiotic stresses in Setaria viridis. *Sci. Rep.* 9, 4028–4116. doi:10.1038/s41598-019-40623-5

Fan, W., Zhao, M., Li, S., Bai, X., Li, J., Meng, H., et al. (2018). Correction to: contrasting transcriptional responses of PYR1/PYL/RCAR ABA receptors to ABA or dehydration stress between maize seedling leaves and roots. *BMC Plant Biol.* 18, 73. doi:10.1186/s12870-018-1283-8

Farooqi, A. A., Tabassum, S., and Ahmad, A. (2017). MicroRNA-34a: a versatile regulator of myriads of targets in different cancers. *Int. J. Mol. Sci.* 18, 2089. doi:10.3390/ijms18102089

Gasteiger, E., Hoogland, C., Gattiker, A., Duvaud, S., Wilkins, M. R., Appel, R. D., et al. (2005). *Protein identification and analysis tools on the ExPASy server BT - the proteomics protocols handbook.* Editor J. M. Walker (Totowa, NJ: Humana Press), 571–607. doi:10.1385/1-59259-890-0:571

Gaut, B. S., Morton, B. R., McCaig, B. C., and Clegg, M. T. (1996). Substitution rate comparisons between grasses and palms: synonymous rate differences at the nuclear gene Adh parallel rate differences at the plastid gene rbcL. *Proc. Natl. Acad. Sci. U. S. A.* 93, 10274–10279. doi:10.1073/pnas.93.19.10274

Gonzalez-Guzman, M., Pizzio, G. A., Antoni, R., Vera-Sirera, F., Merilo, E., Bassel, G. W., et al. (2012). Arabidopsis PYR/PYL/RCAR receptors play a major role in quantitative regulation of stomatal aperture and transcriptional response to abscisic acid. *Plant Cell* 24, 2483–2496. doi:10.1105/tpc.112.098574

González-Guzmán, M., Rodríguez, L., Lorenzo-Orts, L., Pons, C., Sarrión-Perdigones, A., Fernández, M. A., et al. (2014). Tomato PYR/PYL/RCAR abscisic acid receptors show high expression in root, differential sensitivity to the abscisic acid agonist quinabactin, and the capability to enhance plant drought resistance. *J. Exp. Bot.* 65, 4451–4464. doi:10.1093/jxb/eru219

Goodstein, D. M., Shu, S., Howson, R., Neupane, R., Hayes, R. D., Fazo, J., et al. (2012). Phytozome: a comparative platform for green plant genomics. *Nucleic Acids Res.* 40, D1178–D1186. doi:10.1093/nar/gkr944

Goron, T. L., and Raizada, M. N. (2015). Genetic diversity and genomic resources available for the small millet crops to accelerate a New Green Revolution. *Front. Plant Sci.* 6, 157. doi:10.3389/fpls.2015.00157

Guo, D., Zhou, Y., Li, H. L., Zhu, J. H., Wang, Y., Chen, X. T., et al. (2017). Identification and characterization of the abscisic acid (ABA) receptor gene family and its expression in response to hormones in the rubber tree. *Sci. Rep.* 7, 45157–45210. doi:10.1038/srep45157

Guo, Z., Kuang, Z., Wang, Y., Zhao, Y., Tao, Y., Cheng, C., et al. (2020). PmiREN: a comprehensive encyclopedia of plant miRNAs. *Nucleic Acids Res.* 48, D1114–D1121. doi:10.1093/nar/gkz894

Gupta, S. M., Arora, S., Mirza, N., Pande, A., Lata, C., Vasconcelos, M. W., et al. (2017). Finger millet: a "certain" crop for an "uncertain" future and a solution to food insecurity and hidden hunger under stressful environments. *Front. Plant Sci.* 8, 643. doi:10.3389/fpls.2017.00643

Hao, Q., Yin, P., Li, W., Wang, L., Yan, C., Lin, Z., et al. (2011). The molecular basis of ABA-independent inhibition of PP2Cs by a subclass of PYL proteins. *Mol. Cell* 42, 662–672. doi:10.1016/j.molcel.2011.05.011

Hatakeyama, M., Aluri, S., Balachadran, M. T., Sivarajan, S. R., Patrignani, A., Grüter, S., et al. (2018). Multiple hybrid *de novo* genome assembly of finger millet, an orphan allotetraploid crop. *DNA Res. Int. J. rapid Publ. Rep. Genes Genomes* 25, 39–47. doi:10.1093/dnares/dsx036

He, Y., Hao, Q., Li, W., Yan, C., Yan, N., and Yin, P. (2014). Identification and characterization of ABA receptors in oryza sativa. *PLoS One* 9, e95246. doi:10.1371/journal.pone.0095246

Hittalmani, S., Mahesh, H. B., Shirke, M. D., Biradar, H., Uday, G., Aruna, Y. R., et al. (2017). Genome and Transcriptome sequence of Finger millet (*Eleusine coracana* (L.) Gaertn.) provides insights into drought tolerance and nutraceutical properties. *BMC Genomics* 18, 465–516. doi:10.1186/s12864-017-3850-z

Horton, P., Park, K.-J., Obayashi, T., Fujita, N., Harada, H., Adams-Collier, C. J., et al. (2007). WoLF PSORT: protein localization predictor. *Nucleic Acids Res.* 35, W585–W587. doi:10.1093/nar/gkm259

Kim, H., Hwang, H., Hong, J.-W., Lee, Y.-N., Ahn, I. P., Yoon, I. S., et al. (2012). A rice orthologue of the ABA receptor, OsPYL/RCAR5, is a positive regulator of the ABA signal transduction pathway in seed germination and early seedling growth. *J. Exp. Bot.* 63, 1013–1024. doi:10.1093/jxb/err338

Kim, H., Lee, K., Hwang, H., Bhatnagar, N., Kim, D.-Y., Yoon, I. S., et al. (2014). Overexpression of PYL5 in rice enhances drought tolerance, inhibits growth, and modulates gene expression. *J. Exp. Bot.* 65, 453–464. doi:10.1093/jxb/ert397

Larkin, M. A., Blackshields, G., Brown, N. P., Chenna, R., Mcgettigan, P. A., McWilliam, H., et al. (2007). Clustal W and clustal X version 2.0. *Bioinformatics* 23, 2947–2948. doi:10.1093/bioinformatics/btm404

Laskowski, R. A., Jabłońska, J., Pravda, L., Vařeková, R. S., and Thornton, J. M. (2018). PDBsum: structural summaries of PDB entries. *Protein Sci.* 27, 129–134. doi:10.1002/pro.3289

Lei, P., Wei, X., Gao, R., Huo, F., Nie, X., Tong, W., et al. (2021). Genome-wide identification of PYL gene family in wheat: evolution, expression and 3D structure analysis. *Genomics* 113, 854–866. doi:10.1016/j.ygeno.2020.12.017

Lescot, M., Déhais, P., Thijs, G., Marchal, K., Moreau, Y., Van de Peer, Y., et al. (2002). PlantCARE, a database of plant cis-acting regulatory elements and a portal to tools for *in silico* analysis of promoter sequences. *Nucleic Acids Res.* 30, 325–327. doi:10.1093/nar/30.1.325

Lynch, M., and Force, A. (2000). The probability of duplicate gene preservation by subfunctionalization. *Genetics* 154, 459–473. doi:10.1093/genetics/154.1.459

Ma, Y., Szostkiewicz, I., Korte, A., Moes, D., Yang, Y., Christmann, A., et al. (2009). Regulators of PP2C phosphatase activity function as abscisic acid sensors. *Science* 324, 1064–1068. doi:10.1126/science.1172408

McCormick, R. F., Truong, S. K., Sreedasyam, A., Jenkins, J., Shu, S., Sims, D., et al. (2018). The Sorghum bicolor reference genome: improved assembly, gene annotations, a transcriptome atlas, and signatures of genome organization. *Plant J.* 93, 338–354. doi:10.1111/tpj.13781

Meher, P. K., Sahu, T. K., Gupta, A., Kumar, A., and Rustgi, S. (2024). ASRpro: a machine-learning computational model for identifying proteins associated with multiple abiotic stress in plants. *Plant Genome* 17, 202599–e20313. doi:10.1002/tpg2.20259

Merlot, S., Gosti, F., Guerrier, D., Vavasseur, A., and Giraudat, J. (2001). The ABI1 and ABI2 protein phosphatases 2C act in a negative feedback regulatory loop of the abscisic acid signalling pathway. *Plant J.* 25, 295–303. doi:10.1046/j.1365-313X.2001.00965.x

Moore, R. C., and Purugganan, M. D. (2005). The evolutionary dynamics of plant duplicate genes. *Curr. Opin. Plant Biol.* 8, 122–128. doi:10.1016/j.pbi.2004.12.001

Mukami, A., Ngetich, A., Mweu, C., Oduor, R. O., Muthangya, M., and Mbinda, W. M. (2019). Differential characterization of physiological and biochemical responses during drought stress in finger millet varieties. *Physiol. Mol. Biol. Plants* 25, 837–846. doi:10.1007/s12298-019-00679-z

Muthamilarasan, M., Khandelwal, R., Yadav, C. B., Bonthala, V. S., Khan, Y., and Prasad, M. (2014). Identification and molecular characterization of MYB transcription factor superfamily in C4 model plant foxtail millet (*Setaria italica* L.). *PLoS One* 9, e109920. doi:10.1371/journal.pone.0109920

Oliveros, J. C. (2016). Venny 2.1. 0. Venny. An interact tool comp list with venn's diagrams. Available online at: https//bioinfogp.cnb.csic.es/tools/venny/ (Accessed February 15, 2016).

Park, S., Fung, P., Nishimura, N., Jensen, D. R., Zhao, Y., Lumba, S., et al. (2010). Abscisic acid inhibits type 2C protein phosphatases via the PYR/PYL family of START proteins. *Science* 324, 1068–1071. doi:10.1126/science.1173041.Abscisic

Park, S. Y., Fung, P., Nishimura, N., Jensen, D. R., Fujii, H., Zhao, Y., et al. (2009). Abscisic acid inhibits type 2C protein phosphatases via the PYR/PYL family of START proteins. *Science* 324, 1068–1071. doi:10.1126/science.1173041

Paul, S., Markiel, A., Owen, O., Baliga, N. S., Wang, J. T., Ramage, D., et al. (1971). Cytoscape: a software environment for integrated models. *Genome Res.* 13, 426. doi:10.1101/gr.1239303.metabolite

Pizzio, G. A., Rodriguez, L., Antoni, R., Gonzalez-Guzman, M., Yunta, C., Merilo, E., et al. (2013). The PYL4 A194T mutant uncovers a key role of PYR1-LIKE4/PROTEIN PHOSPHATASE 2CA interaction for abscisic acid signaling and plant drought resistance. *Plant Physiol.* 163, 441–455. doi:10.1104/pp.113.224162

Qin, B., Fan, S., Yu, H. Y., Lu, Y. X., and Wang, L. F. (2022). HbMYB44, a rubber tree MYB transcription factor with versatile functions in modulating multiple phytohormone signaling and abiotic stress responses. *Front. Plant Sci.* 13, 893896–893913. doi:10.3389/fpls.2022.893896

Radauer, C., Lackner, P., and Breiteneder, H. (2008). The Bet v 1 fold: an ancient, versatile scaffold for binding of large, hydrophobic ligands. *BMC Evol. Biol.* 8, 286. doi:10.1186/1471-2148-8-286

Rakkammal, K., Maharajan, T., Shriram, R. N., Ram, P. S. J., Ceasar, S. A., and Ramesh, M. (2023a). Physiological, biochemical and molecular responses of finger millet (Eleusine coracana) genotypes exposed to short-term drought stress induced by PEG-6000. *South Afr. J. Bot.* 155, 45–59. doi:10.1016/j.sajb.2023.01.053

Rakkammal, K., Pandian, S., Maharajan, T., Antony, S., Sohn, S. I., and Ramesh, M. (2023b). Humic acid regulates gene expression and activity of antioxidant enzymes to inhibit the salt - induced oxidative stress in finger millet. *Cereal Res. Commun.* 52, 397–411. doi:10.1007/s42976-023-00429-8

Rani, V., Joshi, D. C., Joshi, P., Singh, R., and Yadav, D. (2023). "Millet Models" for harnessing nuclear factor-Y transcription factors to engineer stress tolerance in plants: current knowledge and emerging paradigms. *Planta* 258, 29. doi:10.1007/s00425-023-04186-0

Rani, V., Rana, S., Muthamilarasan, M., Joshi, D. C., and Yadav, D. (2024a). Expression profiling of Nuclear Factor-Y (NF-Y) transcription factors during dehydration and salt stress in finger millet reveals potential candidate genes for multiple stress tolerance. *Planta* 259, 136. doi:10.1007/s00425-024-04417-y

Rani, V., Singh, V. K., Joshi, D. C., Singh, R., and Yadav, D. (2024b). Genome-wide identification of nuclear factor -Y (NF-Y) transcription factor family in finger millet reveals structural and functional diversity. *Heliyon* 10, e36370. doi:10.1016/j.heliyon.2024.e36370

Rani, V., Singh, V. K., Joshi, D. C., Singh, R., and Yadav, D. (2024c). Molecular docking insights into nuclear factor Y (NF-Y) transcription factor and pyrabactin resistance 1 (PYL) receptor proteins reveal abiotic stress regulation in finger millet. *Crop Des.* 3, 100051. doi:10.1016/j.cropd.2023.100051

Romero, P., Lafuente, M. T., and Rodrigo, M. J. (2012). The Citrus ABA signalosome: identification and transcriptional regulation during sweet orange fruit ripening and leaf dehydration. *J. Exp. Bot.* 63, 4931–4945. doi:10.1093/jxb/ers168

Sanjay Kumar, T., Nageswari, R., Somasundaram, S., Anantharaju, P., Baskar, M., Ramesh, T., et al. (2024). Significance of millets for food and nutritional security—an overview. *Discov. Food* 4, 73. doi:10.1007/s44187-024-00149-w

Santiago, J., Dupeux, F., Betz, K., Antoni, R., Gonzalez-Guzman, M., Rodriguez, L., et al. (2012). Structural insights into PYR/PYL/RCAR ABA receptors and PP2Cs. *Plant Sci.* 182, 3–11. doi:10.1016/j.plantsci.2010.11.014

Santiago, J., Rodrigues, A., Saez, A., Rubio, S., Antoni, R., Dupeux, F., et al. (2009). Modulation of drought resistance by the abscisic acid receptor PYL5 through inhibition of clade A PP2Cs. *Plant J.* 60, 575–588. doi:10.1111/j.1365-313X.2009.03981.x

Shin, R., Burch, A. Y., Huppert, K. A., Tiwari, S. B., Murphy, A. S., Guilfoyle, T. J., et al. (2007). The Arabidopsis transcription factor MYB77 modulates auxin signal transduction. *Plant Cell* 19, 2440–2453. doi:10.1105/tpc.107.050963

Sood, S., Joshi, D. C., Chandra, A. K., and Kumar, A. (2019). Phenomics and genomics of finger millet: current status and future prospects. *Planta* 250, 731–751. doi:10.1007/s00425-019-03159-6

Szklarczyk, D., Gable, A. L., Nastou, K. C., Lyon, D., Kirsch, R., Pyysalo, S., et al. (2021). The STRING database in 2021: customizable protein-protein networks, and functional characterization of user-uploaded gene/measurement sets. *Nucleic Acids Res.* 49, D605–D612. doi:10.1093/nar/gkaa1074

Tähtiharju, S., Heino, P., and Palva, E. T. (2002). *ATPP2CA negatively regulates ABA responses during cold acclimation and interacts with the potassium channel AKT3 BT - plant cold hardiness: gene regulation and genetic engineering.* Editors P. H. Li and E. T. Palva (Boston, MA: Springer US), 55–62. doi:10.1007/978-1-4615-0711-6_5

Talwar, H. S., Kumar, S., Madhusudhana, R., Nanaiah, G. K., Ronanki, S., and Tonapi, V. A. (2020). Variations in drought tolerance components and their association with yield components in finger millet (Eleusine coracana). *Funct. Plant Biol.* 47, 659–674. doi:10.1071/FP19274

Tamura, K., Stecher, G., and Kumar, S. (2021). MEGA11: molecular evolutionary genetics analysis version 11. *Mol. Biol. Evol.* 38, 3022–3027. doi:10.1093/molbev/msab120

Wang, Y.-G., Fu, F.-L., Yu, H.-Q., Hu, T., Zhang, Y.-Y., Tao, Y., et al. (2018). Interaction network of core ABA signaling components in maize. *Plant Mol. Biol.* 96, 245–263. doi:10.1007/s11103-017-0692-7

Waterhouse, A., Bertoni, M., Bienert, S., Studer, G., Tauriello, G., Gumienny, R., et al. (2018). SWISS-MODEL: homology modelling of protein structures and complexes. *Nucleic Acids Res.* 46, W296–W303. doi:10.1093/nar/gky427

Wenkel, S., Turck, F., Singer, K., Gissot, L., Le Gourrierec, J., Samach, A., et al. (2006). CONSTANS and the CCAAT box binding complex share a functionally important domain and interact to regulate flowering of Arabidopsis. *Plant Cell* 18, 2971–2984. doi:10.1105/tpc.106.043299

Wu, C., Zhang, M., Liang, Y., Zhang, L., and Diao, X. (2023). Salt stress responses in foxtail millet: physiological and molecular regulation. *Crop J.* 11, 1011–1021. doi:10.1016/j.cj.2023.06.001

Xiong, L., Schumaker, K. S., and Zhu, J.-K. (2002). Cell signaling during cold, drought, and salt stress. *Plant Cell* 14, S165–S183. doi:10.1105/tpc.000596

Yadav, S. K., Santosh Kumar, V. V., Verma, R. K., Yadav, P., Saroha, A., Wankhede, D. P., et al. (2020). Genome-wide identification and characterization of ABA receptor PYL gene family in rice. *BMC Genomics* 21, 676–727. doi:10.1186/s12864-020-07083-y

Yin, P., Fan, H., Hao, Q., Yuan, X., Wu, D., Pang, Y., et al. (2009). Structural insights into the mechanism of abscisic acid signaling by PYL proteins. *Nat. Struct. Mol. Biol.* 16, 1230–1236. doi:10.1038/nsmb.1730

Yu, J., Hu, S., Wang, J., Wong, G. K. S., Li, S., Liu, B., et al. (2002). A draft sequence of the rice genome (Oryza sativa L. ssp. indica). *Science* 296, 79–92. doi:10.1126/science.1068037

Yu, T.-F., Liu, Y., Fu, J.-D., Ma, J., Fang, Z.-W., Chen, J., et al. (2021). The NF-Y-PYR module integrates the abscisic acid signal pathway to regulate plant stress tolerance. *Plant Biotechnol. J.* 19, 2589–2605. doi:10.1111/pbi.13684

Yue, E., Li, C., Li, Y., Liu, Z., and Xu, J. H. (2017). MiR529a modulates panicle architecture through regulating SQUAMOSA PROMOTER BINDING-LIKE genes in rice (Oryza sativa). *Plant Mol. Biol.* 94, 469–480. doi:10.1007/s11103-017-0618-4

Zhang, G., Liu, X., Quan, Z., Cheng, S., Xu, X., Pan, S., et al. (2012). Genome sequence of foxtail millet (Setaria italica) provides insights into grass evolution and biofuel potential. *Nat. Biotechnol.* 30, 549–554. doi:10.1038/nbt.2195

Zhang, Z., Li, J., Zhao, X.-Q., Wang, J., Wong, G. K.-S., and Yu, J. (2006). KaKs_Calculator: calculating Ka and Ks through model selection and model averaging. *Genomics. Proteomics Bioinforma.* 4, 259–263. doi:10.1016/S1672-0229(07)60007-2

Zhu, J. (2016). Abiotic stress signaling and responses in plants. *Cell* 167, 313–324. doi:10.1016/j.cell.2016.08.029

Zhu, J.-K. (2002). Salt and drought stress signal transduction in plants. *Annu. Rev. Plant Biol.* 53, 247–273. doi:10.1146/annurev.arplant.53.091401.143329